Supporting Information for

Integrated "all-in-one" strategy to construct highly efficient Pd catalyst for CO_2 transformation

Lingfang Kong,[+a] Zekun Tao,[+a] Yunjia Li,[a] Huiwen Gong,[a] Yun Bai,[a] Longbin Li,[a] Xianjin Zhang,[b] Zhonggao Zhou*[a] and Yiwang Chen*[a]

* Corresponding authors

[a] College of Chemistry and Chemical Engineering/Analysis and Testing Center/Key Laboratory of Jiangxi University for Functional Materials Chemistry, Gannan Normal University, Ganzhou 341000, P. R. China
E-mail: zhgzhou@foxmail.com, ywchen@ncu.edu.cn

[b] Institute of Chemistry Education, Fujian Institute of Education, Fuzhou 350025, P. R. China

[+] L. Kong and Z. Tao contributed equally to this work

Table of Contents

1. Experimental Section

1.1 General

All nuclear magnetic resonance (NMR) spectra were acquired using a Bruker Advance III 400 NMR spectrometer, with chemical shifts (δ) reported in ppm. Fourier-transform infrared (FT-IR) spectra were recorded on an Avatar Nicolet FT-IR spectrometer either neat with smart OMNI-transmission accessories or with KBr pellets using standard methods, with frequencies reported in cm^{-1}. Liquid chromatography–high–resolution mass spectrometry (LC-HR/MS) spectra were obtained using a Waters G2-XS QTOF mass spectrometer, with samples dissolved in methanol. X-ray photoelectron Spectrometer (XPS) measurements were conducted on an ESCALAB 250Xi X-ray photoelectron spectrometer (Thermo Fisher) using an Al *Ka* source (15 kV, 10 mA) with Ar etching for 30 min (the charge of C-C carbon species here was corrected to 284.8 eV).

All reagents were commercially sourced from Sinopharm Chemical Reagent Limited Corporation or Shanghai Aladdin Biochemical Technology Co., Ltd., and used without further purification unless specified otherwise. CO_2 (CO_2, 99.99%) and simulated flue gas (CO_2/N_2, Vol/Vol = 15:85) were procured from Ganzhou Shengda Gas Co., Ltd. Flash column chromatography was carried out using silica gel (300-400 mesh).

1.2 Synthesis and Characterization of Imidazolium Salts

Synthesis of Im-Br1-4

2-Bromoethyl glucoside (2.5 equivalent) and *N*-alkylated imidazole (1.0 equivalent) were dissolved in anhydrous acetonitrile and the solution was heated at 120°C for 48 hours. Upon cooling, the acetonitrile was evaporated using a rotary evaporator. Purification was achieved by column chromatography on silica gel using a gradient elution of dichloromethane/methanol (V:V = 20:1 to 10:1), resulting in the isolation of products Im-Br**1-4** (84-96%) as pale yellow solids.

Synthesis of Im-Br5

Im-Br**1** (0.131 g, 1.0 mmol) was dissolved in anhydrous methanol (10 mL) and reacted with a catalytic quantity of freshly prepared sodium methoxide (NaOMe) to achieve a basic environment, maintaining a pH of about 9.0. The solution was stirred at room temperature (RT) overnight. Subsequent neutralization was carried out using dry Amberlite IR 120 (H^+) resin to achieve a pH of around 7.0. The crude mixture underwent simple washing successively with $NaHCO_3$, NaCl, and H_2O. Solvent evaporation gave the product Im-Br**5** (95%) as a pale yellow viscous liquid.

Synthesis of Cat1-5

In a 100 mL round-bottom flask, Im-Br**1** (0.131 g, 0.10 mmol) were dissolved in 50.0 mL of dichloromethane, and aqueous solution of sodium tetrachloropalladate (0.01 g·mL^{-1}, 4.4 mL) was added in the flask and the mixture was stirred at RT overnight. The solution was washed twice with ultrapure water, then removed by rotary evaporation and dried under vacuum to get the product Cat**1** (0.123 g, 92%) as a reddish brown solid. Cat**2-4** were prepared in a similar method of that for Cat**1**. Cat**2-4** absorb moisture easily and followed the trend of the other palladium salts, being reddish brown.

Im-Br**1**, 75%, ^{1}H NMR (400 MHz, $CDCl_3$) δ 10.41 (s, 2H), 7.72 (dd, J = 12.6, 7.6 Hz, 4H), 7.53 (s, 4H), 7.42 (t, J = 12.4 Hz, 4H), 5.70 (s, 2H), 5.18 (s, 2H), 4.99 (t, J = 9.4 Hz, 2H), 4.83 (t, J = 9.6 Hz, 4H), 4.72 – 4.66 (m, 4H), 4.55 (d, J = 7.9 Hz, 2H), 4.23 (s, 2H), 4.10 (d, J = 5.0 Hz, 1H), 4.03 (s, 1H), 3.94 (d, J = 11.2 Hz, 2H), 3.67 (d, J = 9.5 Hz, 2H), 3.17 (s, 2H), 1.90 – 1.80 (m, 20H), 1.53 (s, 4H) ppm; ^{13}C NMR (101 MHz, $CDCl_3$) δ 170.6, 169.9, 169.4, 169.3, 142.4, 133.4, 132.1, 130. 8, 130.1, 127.2, 127.0, 114.3, 113.5, 100.0, 72.5, 71.6, 70.8, 68.0, 61.6, 53.6, 50.6, 49.9, 47.8, 20.8, 20.5, 20.5, 20.4 ppm. FT-IR (cm^{-1}): 3422.78, 3029.74, 2959.65, 1749.14, 1629.30, 1564.71, 1431.76, 1374.37, 1227.92, 1038.52, 909.18, 756.04, 604.81, 544.35, 433.80. HR-MS m/z: $[M-Br]^{2+}$ calcd for $C_{54}H_{64}N_4O_{20}$, 544.20515; found 544.20352.

Im-Br**2**, 80%, ^1H NMR (400 MHz, $CDCl_3$) δ 9.78 (s, 2H), 7.74 (s, 2H), 7.54 (s, 4H), 7.49 (s, 2H), 5.57 (s, 4H), 5.16 (t, *J* = 9.5 Hz, 2H), 4.99 (t, *J* = 9.7 Hz, 2H), 4.88 (dd, *J* = 9.6, 8.1 Hz, 2H), 4.64 (dd, *J* = 18.1, 5.8 Hz, 4H), 4.58 – 4.51 (m, 2H), 4.19 (dd, *J* = 12.5, 4.5 Hz, 3H), 4.12 (dd, *J* = 16.9, 6.5 Hz, 3H), 4.00 (dd, *J* = 9.6, 6.2 Hz, 2H), 3.81 – 3.76 (m, 2H), 2.04 (s, 4H), 1.97 (d, *J* = 8.5 Hz, 20H) ppm; ^{13}C NMR (101 MHz, $CDCl_3$) δ 170.8, 170.2, 169.9, 169.7, 137.0, 134.4, 130.5, 123.6, 122.5, 100.5, 72.6, 72.1, 71.3, 68.5, 67.9, 62.0, 52.9, 50.0, 21.1, 20.8 ppm. FT-IR (cm^{-1}): 3422.68, 3142.06, 3094.39, 2959.81, 1749.10, 1633.94, 1563.48, 1436.24, 1373.71, 1228.29, 1163.63, 1039.94, 909.73, 840.19, 729.27, 603.28, 419.63. HR-MS m/z: $[M-Br]^{2+}$ calcd for $C_{48}H_{64}N_4O_{20}$, 494.18950; found, 494.18950.

Im-Br**3**, 85%, ^1H NMR (400 MHz, $CDCl_3$) δ 7.70 (d, *J* = 3.2 Hz, 4H), 7.44 (s, 4H), 5.67 – 5.42 (m, 4H), 5.19 – 5.12 (m, 2H), 5.05 (s, 1H), 4.98 (t, *J* = 8.6 Hz, 2H), 4.83 – 4.77 (m, 2H), 4.67 (s, 3H), 4.57 (d, *J* = 7.8 Hz, 3H), 4.22 (s, 1H), 4.14 – 4.06 (m, 4H), 3.83 (d, *J* = 6.0 Hz, 2H), 3.49 – 3.29 (m, 2H), 2.70 (s, 6H), 2.05 (d, *J* = 8.4 Hz, 6H), 2.01 – 1.96 (m, 14H), 1.94 (s, 4H) ppm; ^{13}C NMR (101 MHz, $CDCl_3$) δ 170.9, 170.2, 169.8, 145.4, 134.4, 129.5, 122.4, 100.5, 72.7, 72.1, 71.3, 68.5, 68.2, 62.0, 53.7, 51.7, 48.9, 21.1, 20.8, 11.4 ppm. FT-IR (cm^{-1}): 3432.60, 2958.18, 1748.75, 1632.64, 1531.70, 1429.29, 1375.24, 1229.56, 1038.05, 910.28, 749.72, 599.75, 550.80, 408.41. HR-MS m/z: $[M-Br]^{2+}$ calcd for $C_{46}H_{60}N_4O_{20}$, 508.20515; found, 508.20855.

Im-Br**4**, 88%, ^1H NMR (400 MHz, DMSO-d_6) δ 10.02 (s, 2H), 8.11 (d, *J* = 8.0 Hz, 2H), 7.93 (d, *J* = 7.8 Hz, 2H), 7.66 (d, *J* = 7.7 Hz, 2H), 7.63 (d, *J* = 8.2 Hz, 2H), 7.56 (s, 4H), 5.78 (s, 4H), 4.51 (t, *J* = 7.2 Hz, 4H), 1.34 – 1.20 (m, 24H), 0.83 (dd, *J* = 8.0, 5.5 Hz, 6H) ppm. ^{13}C NMR (101 MHz, DMSO-*d₆*) δ 143.5, 135.7, 132.4, 131.8, 130.0, 127.7, 115.0, 115.0, 50.4, 49.6, 48.0, 32.2, 29.5, 26.8, 23.1, 14.9 ppm. FT-IR (cm^{-1}): 3129.71, 3043.10, 2926.50, 1748.60, 1661.68, 1612.57, 1561.02, 1518.02, 1463.46, 1422.94, 1379.67, 1345.07, 1263.28, 1215.10, 1194.00, 1131.38, 1019.60, 860.72, 765.03, 684.52, 568.91. HR-MS m/z: [M-Br]$^{2+}$ calcd for $C_{38}H_{52}N_4$, 282.20905; found, 282.21105.

Im-Br**5**, 94%, ^{1}H NMR (400 MHz, DMSO-d_6) δ 10.08 (s, 2H), 8.15 (d, *J* = 7.4 Hz, 2H), 7.96 (d, *J* = 7.4 Hz, 2H), 7.63 (t, *J* = 7.0 Hz, 4H), 7.57 (s, 4H), 5.82 (s, 4H), 5.24 (s, 2H), 5.09 (d, *J* = 30.9 Hz, 2H), 4.77 (s, 3H), 4.68 (s, 1H), 4.24 (d, *J* = 7.8 Hz, 2H), 4.15 – 4.09 (m, 2H), 4.04 – 3.97 (m, 2H), 3.18 – 3.08 (m, 4H), 3.03 (d, *J* = 8.1 Hz, 2H), 2.92 (d, *J* = 7.8 Hz, 2H) ppm; ^{13}C NMR (101 MHz, DMSO-d_6) δ144.5, 135.7, 132.3, 131.7, 123.0, 127.7, 115.2, 114.9, 104.1, 77.9, 77.5, 74.4, 71.0, 67.0, 62.0, 50.4, 48.2 ppm. FT-IR (cm^{-1}): 3388.07, 3130.84, 3060.75, 2965.42, 2922.13, 2853.27, 1742.99, 1632.36, 1557.80, 1515.89, 1452.93, 1372.23, 1344.86, 1287.08, 1218.65,1197.41, 1162.93, 1076.70, 1034.22, 895.34, 863.37, 758.29, 666.36, 566.14. HR-MS m/z: [M-Br]$^{2+}$ calcd for $C_{38}H_{48}N_4O_{12}$, 376.16289; found, 376.16494.

Cat**1**, 92%, ^{1}H NMR (400 MHz, $CDCl_3$) δ 9.88 (s, 2H), 8.06 (s, 4H), 7.87 (s, 4H), 7.60 (s, 4H), 5.89 (s, 3H), 5.30 (s, 1H), 5.12 (d, *J* = 9.1 Hz, 2H), 4.96 (d, *J* = 9.7 Hz, 4H), 4.90 – 4.78 (m, 4H), 4.70 (d, *J* = 7.1 Hz, 2H), 4.48 (s, 2H), 4.34 (s, 2H), 4.21 (d, *J* = 9.6 Hz, 2H), 4.09 (d, *J* = 10.8 Hz, 2H), 3.84 (s, 2H), 1.97 (d, *J* = 15.9 Hz, 20H), 1.70 (s, 4H) ppm; ^{13}C NMR (101 MHz, $CDCl_3$) δ 170.9, 170.2, 169.8, 142.2, 133.9, 132.6, 131.3, 130.9, 127.8, 114.8, 114.1, 100.5, 73.0, 72.0, 71.3, 68.5, 68.4, 62.0, 53.7, 51.4, 48.5, 21.2, 20.9, 20.9, 20.8 ppm. FT-IR (cm^{-1}): 3441.45, 2960.63, 1749.56, 1628.39, 1565.79, 1427.51, 1372.95, 1227.05, 1035.94, 749.83, 700.59, 599.07, 538.82, 430.84. HR-MS m/z: [M-$PdCl_4$]$^{2+}$ calcd for $C_{54}H_{64}N_4O_{20}$, 544.20515; found 544.20901.

Cat**2**, 98%, ^{1}H NMR (400 MHz, $CDCl_3$) δ 9.35 (s, 2H), 7.93 (s, 4H), 7.62 (s, 2H), 7.51 (s, 2H), 5.68 (s, 3H), 5.29 (s, 1H), 5.18 (t, *J* = 9.2 Hz, 2H), 5.02 (t, *J* = 9.2 Hz, 2H), 4.91 (t, *J* = 8.1 Hz, 2H), 4.74 (d, *J* = 6.8 Hz, 4H), 4.59 (s, 2H), 4.31 (s, 2H), 4.23 (s, 4H), 4.16 (d, *J* = 11.5 Hz, 2H), 3.88 (d, *J* = 7.8 Hz, 2H), 2.01 (t, *J* = 15.8 Hz, 24H) ppm; ^{13}C NMR (101 MHz, $CDCl_3$) δ 170.9, 170.2, 170.0, 169.8, 136.6, 134.5, 130.9, 124.1, 122.8, 100.5, 72.7, 72.0, 71.4, 68.41, 68.2, 62.0, 53.7, 53.5, 50.5, 21.4, 21.3, 20.9 ppm. FT-IR (cm^{-1}): 3494, 3146, 2968, 1956, 1629, 1582, 1533, 1431, 1376, 1226, 1171, 1035, 912, 755, 604. HR-MS m/z: $[M\text{-}PdCl_4]^{2+}$ calcd for $C_{48}H_{64}N_4O_{20}$, 494.18950; found, 494.19304.

Cat**3**, 98%, ^{1}H NMR (400 MHz, $CDCl_3$) δ 7.71 (s, 4H), 7.65 (s, 2H), 7.60 (s, 2H), 5.65 (t, *J* = 17.8 Hz, 4H), 5.20 (t, *J* = 9.4 Hz, 2H), 5.04 (t, *J* = 9.6 Hz, 2H), 4.90 (t, *J* = 8.7 Hz, 2H), 4.75 (d, *J* = 7.7 Hz, 2H), 4.64 (s, 4H), 4.36 (s, 2H), 4.31 – 4.19 (m, 4H), 4.15 (d, *J* = 11.4 Hz, 2H), 3.89 (d, *J* = 9.3 Hz, 2H), 2.90 (s, 6H), 2.10 (s, 6H), 2.02 (d, *J* = 9.5 Hz, 18H) ppm; ^{13}C NMR (101 MHz, $CDCl_3$) δ 171.0, 170.3, 170.0, 169.9, 145.4, 134.2, 130.1, 122.9, 122.5, 100.5, 72.9, 72.0, 71.4, 68.5, 68.2, 62.0, 52.5, 49.5, 21.4, 21.3, 21.0, 12.0 ppm. FT-IR (cm^{-1}): 3480, 3146, 3105, 2968, 2934, 2860, 1752, 1629, 1561, 1431, 1377, 1226, 1165, 1042, 987, 912, 803, 727, 604. HR-MS m/z: $[M\text{-}PdCl_4]^{2+}$ calcd for $C_{46}H_{60}N_4O_{20}$, 508.20515; found, 508.20871.

Cat**4**, 95%, ^{1}H NMR (400 MHz, DMSO-*d*$_6$) δ 10.01 (s, 2H), 8.10 (d, *J* = 7.9 Hz, 2H), 7.92 (d, *J* = 7.8 Hz, 2H), 7.67 (t, *J* = 5.4 Hz, 2H), 7.63 (d, *J* = 8.2 Hz, 2H), 7.55 (s, 4H), 5.78 (s, 4H), 4.50 (t, *J* = 7.3 Hz, 4H), 1.30 (d, *J* = 3.1 Hz, 8H), 1.23 (d, *J* = 11.0 Hz, 16H), 0.85 – 0.81 (m, 6H) ppm; ^{13}C NMR (101 MHz, DMSO-*d*$_6$) δ 143.5, 135.7, 132.4, 131.9, 129.9, 127.8, 115.0, 114.9, 50.5, 48.0, 32.20, 29.5, 29.5, 29.5, 26.8, 23.1, 15.0 ppm. FT-IR (cm^{-1}): 3124.38, 3027.67, 2955.04, 2923.84, 2852.83, 1717.73, 1633.64, 1613.73, 1456.48, 1422.46, 1340.72, 1261.30, 1261.30, 1215.89, 1179.74, 1094.89, 1018.06, 868.22, 802.31, 752.41, 689.51, 602.02, 570.65. HR-MS m/z: $[M\text{-}PdCl_4]^{2+}$ calcd for $C_{38}H_{52}N_4$, 282.20905; found, 282.21053.

Cat**5**, 97%, ^{1}H NMR (400 MHz, DMSO-*d*$_6$) δ 10.10 (s, 2H), 8.14 (d, *J* = 7.1 Hz, 2H), 7.95 (d, *J* = 7.4 Hz, 2H), 7.67 – 7.59 (m, 4H), 7.57 (s, 4H), 5.82 (s, 4H), 5.27 (d, J = 18.8 Hz, 2H), 5.07 (s, 2H), 4.76 (s, 4H), 4.23 (d, J = 7.7 Hz, 2H), 4.10 (s, 2H), 4.01 (s, 2H), 3.15 (t, J = 8.7 Hz, 2H), 3.12 – 3.07 (m, 2H), 3.03 (d, J = 9.0 Hz, 2H), 2.90 (t, J = 8.2 Hz, 2H) ppm; ^{13}C NMR (101 MHz, DMSO-d_6) δ 144.6, 135.7, 132.3, 131.7, 130.0, 127.8, 115.3, 114.9, 104.1, 77.9, 77.5, 74.4, 71.0, 67.1, 61.9, 50.4, 48.3 ppm. FT-IR (cm^{-1}): 2973.83, 2923.74, 2856.07, 1745.01, 1633.75, 1556.04, 1518.69, 1487.36, 1455.67, 1421.58, 1373.17, 1339.25, 1218.69, 1186.56, 1070.35, 1024.42, 949.53, 856.57, 758.90, 652.34, 599.07, 566.15, 534.58. HR-MS m/z: [M-PdCl$_4$]$^{2+}$ calcd for $C_{38}H_{48}N_4O_{12}$, 376.16289; found, 376.16457.

1.3 Synthesis and Characterization of Propargylic Amines

For the synthesis of propargylic amine **6**, propargyl halide (1.0 mmol) was added dropwise to the corresponding amine (3.0 mmol) at 0°C in the dark, and the mixture was slowly warmed to RT. The reaction was then stirred for 12-24 hours. Subsequently, NaOH and dichloromethane were introduced. After extracting the aqueous layer with dichloromethane, the organic phase was washed with saturated brine, dried over $MgSO_4$, and the solvent was evaporated. The crude product was further purified by flash column chromatography on silica gel using a gradient elution of V_{PE}/V_{EA} = 20:1.

1.4 General Procedure for the Synthesis of Propargylic Amines with CO_2

In a standard procedure, Cat**1** (0.25-0.5 mol%), propargylic amine **6** (0.05 mmol), and NaOAc (0.075 mmol) were combined in DMSO (1.0 mL) within a reaction vessel. A simulated flue gas (CO_2/N_2, Vol/Vol = 15:85, bubbling) was introduced into the preheated reaction mixture using a long hollow needle (φ 0.7 × 200 mm) immersed in a 70°C oil bath. The reaction mixture was then stirred for a specified duration. The yield was quantified using ^{1}H NMR spectroscopy. To determine the isolated yields of purified products, the crude material was concentrated and subjected to purification via column chromatography on silica gel using a gradient elution of petroleum ether/ethyl acetate (V:V = 20:1 to 10:1). The isolated yields were calculated based on the initial reactants.

2. Catalytic Section

2.1 Table S1. Comparison of TOFs with Other Reported Catalysts

Entry	Catalyst	T (°C)/t (h)	*P* (atm)	TOF (h^{-1})	TON	Cycles	Ref.
1	**Cat1**	**70/0.083**	**0.15**	**3456**	**400**	**10**	**Herein**
2	CuI/DBU	50/4	1.0	2	8	/	1
3	AgOAc	25/7	1.0	7	49	/	2
4	$AgNO_3$/DBU	60/2	1.0	94	188	/	3
5	$CoBr_2$/TBD	80/9	1.0	1	9	/	4
6	$ZnCl_2(TBD)_2$	60/12	1.0	2	24	/	5
7	Ag_{27}-MOF	25/6	1.0	16	96	4	6
8	TOS-Ag_4	25/24	1.0	4	96	5	7
9	Zn_{116}	70/12	1.0	31	372	10	8
10	PdSCS	50/0.33	1.0	60	19.8	/	9
11	Ag@TpPa-1	60/18	1.0	17	306	5	10
12	Ag@2,6-FPP-TAPT	50/2	1.0	964	1928	4	11
13	Cu_2O@ZIF-8	40/6	1.0	3.3	19.8	5	12
14	Cu^I/Cu^{II}-MOF	30/0.17	1.0	230	39.1	5	13
15	Pd@BBA-2	40/2	1.0	43.68	87.36	5	14
15	AuCl(IPr)	40/15	1.0	3.0	45	/	15
16	AgCl(IPr)	40/15	1.0	3.0	45	/	16
17	[Au]	RT/24	air	5.33	127.9	/	17
18	Ag-HMP-2	60/20	1.0	10.6	212	/	18

Entry	Catalyst	T (°C)/t (h)	*P* (atm)	TOF (h^{-1})	TON	Cycles	Ref.
19	Ag-MOF-1	RT/24	1.0	0.56	13.44	/	19
20	2G*n*[TEG][Au]	RT/24	1.0	1.77	42.48	/	20
21	AcGlu-Im-$PdCl_4$	70/0.5	0.15	1440	720	/	21
22	Ag_4 NC	25/2	1.0	2873	5746	5	22
23	Cu_6-NH_2	30/1.5	1.0	387	580.5	5	23
24	AcGlu-Im-Br **3**/$CuBr_2$	80/0.33	1.0	400	132	/	24
25	Cu^{I}-TpBD-COF	80/5	1.0	1058	5290	9	25
26	$Cu^{I}Cu^{II}$ DA/WN	40/5	1.0	38.4	192	5	26

3. Characterizations

3.1 Comparative NMR Spectra of Imidazolium Salts

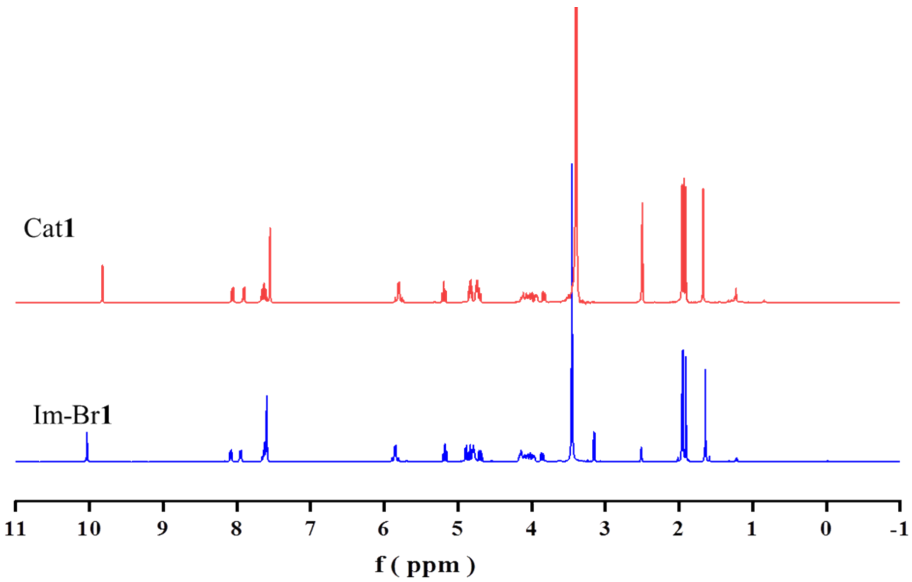

Fig. S1 ^{1}H NMR of Cat**1**/Im-Br**1** in DMSO-d_6.

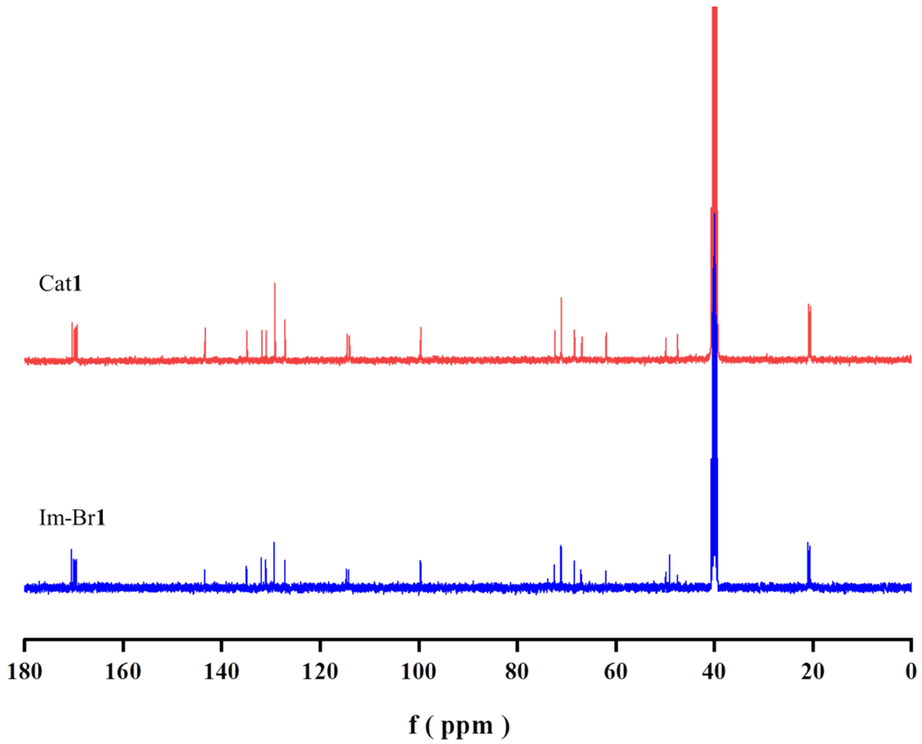

Fig. S2 ^{13}C NMR of Cat**1**/Im-Br**1** in DMSO-d_6.

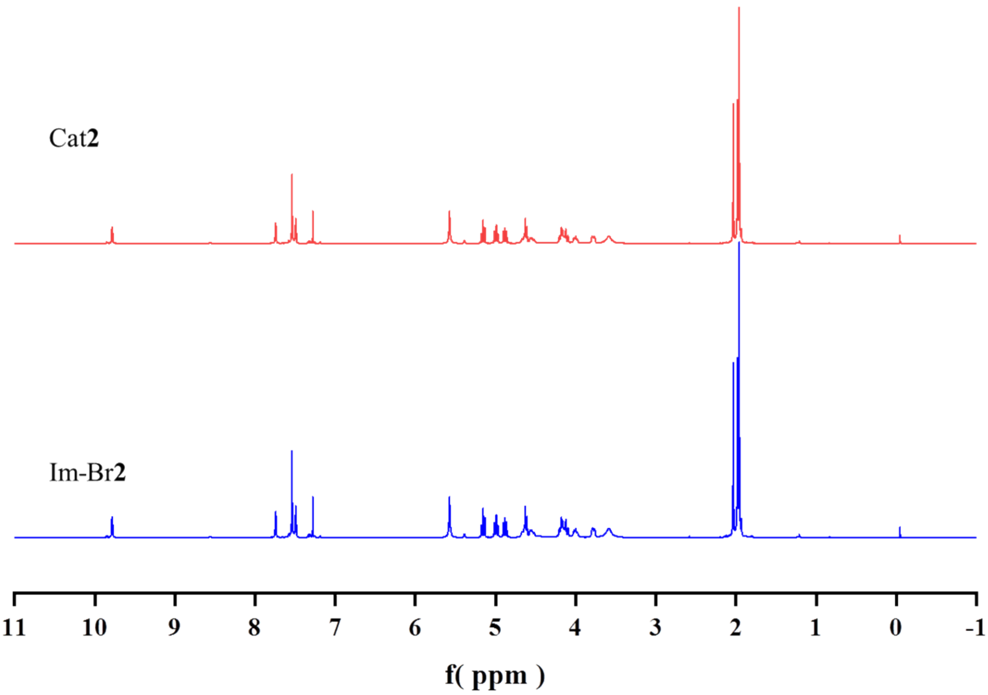

Fig. S3 ^{1}H NMR of Cat**2**/Im-Br**2** in $CDCl_3$.

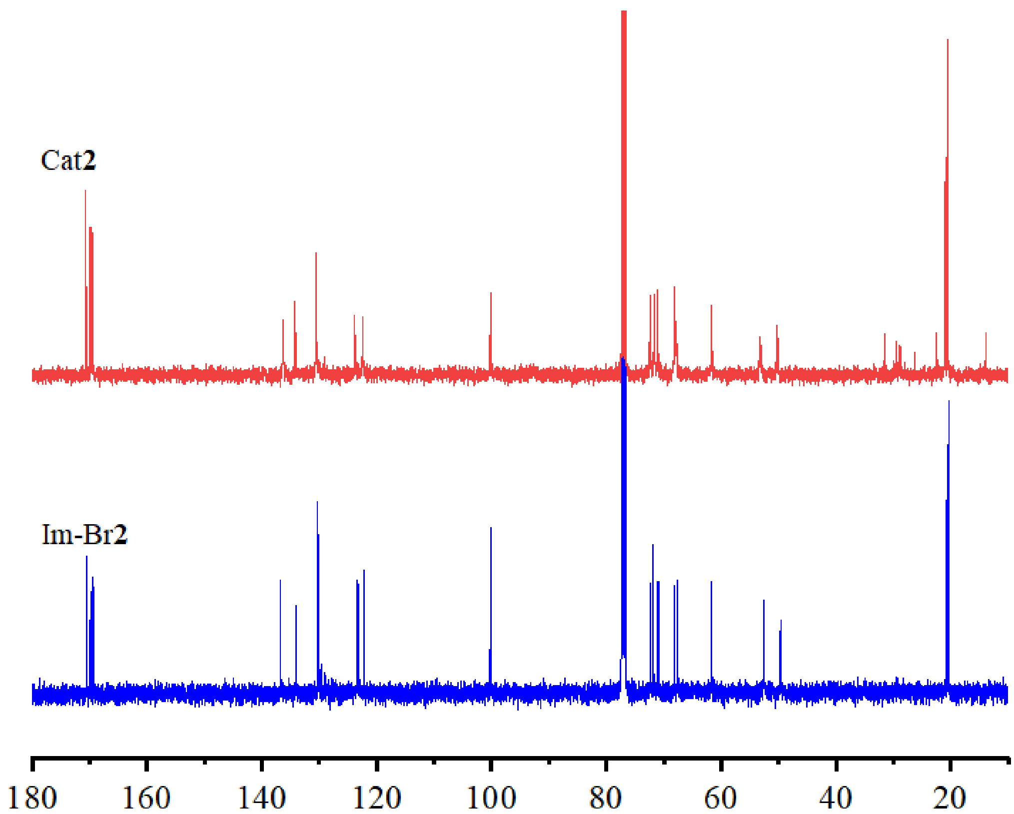

Fig. S4 ^{13}C NMR of Cat**2**/Im-Br**2** in $CDCl_3$.

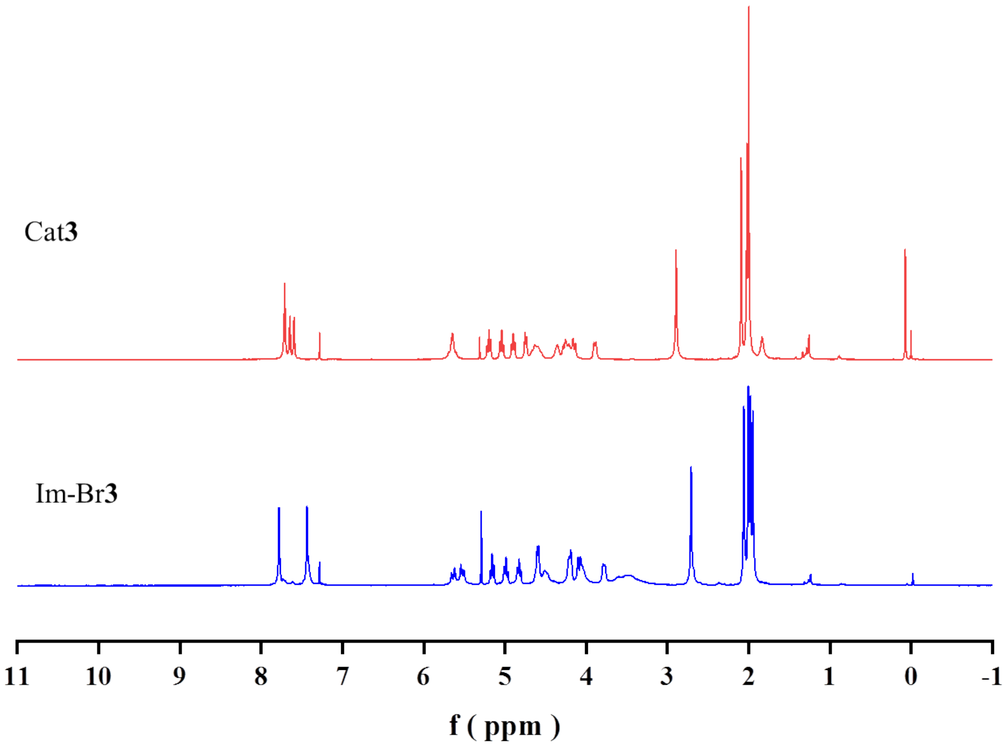

Fig. S5 ¹H NMR of Cat**3**/Im-Br**3** in $CDCl_3$.

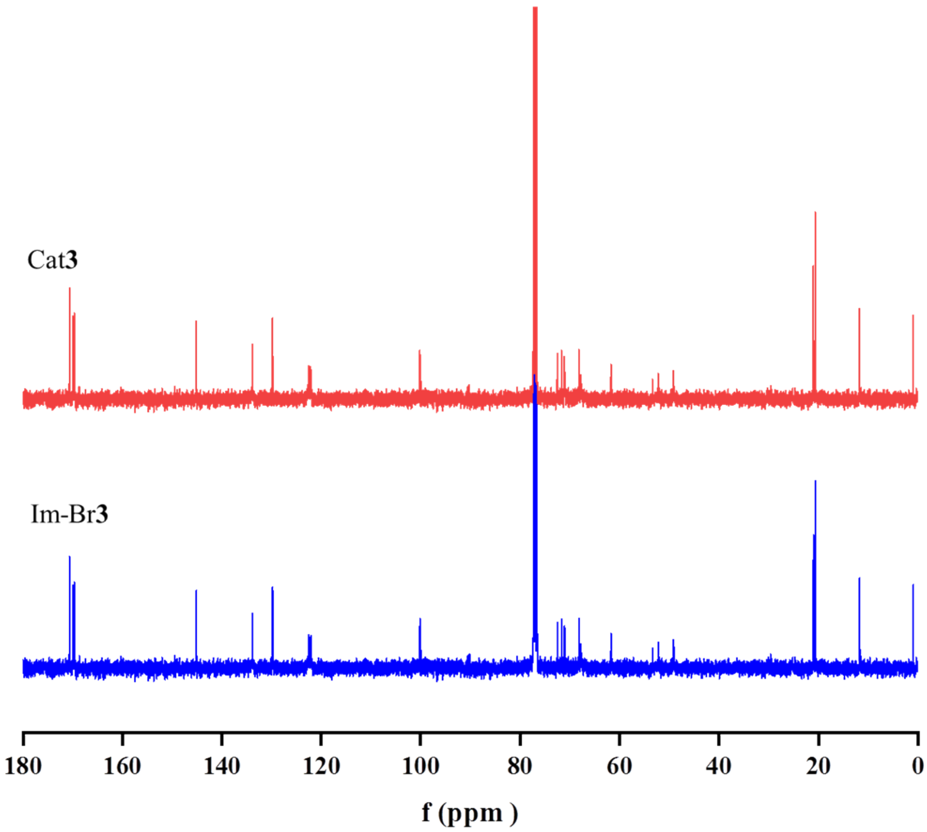

Fig. S6 ¹³C NMR of Cat**3**/Im-Br**3** in $CDCl_3$.

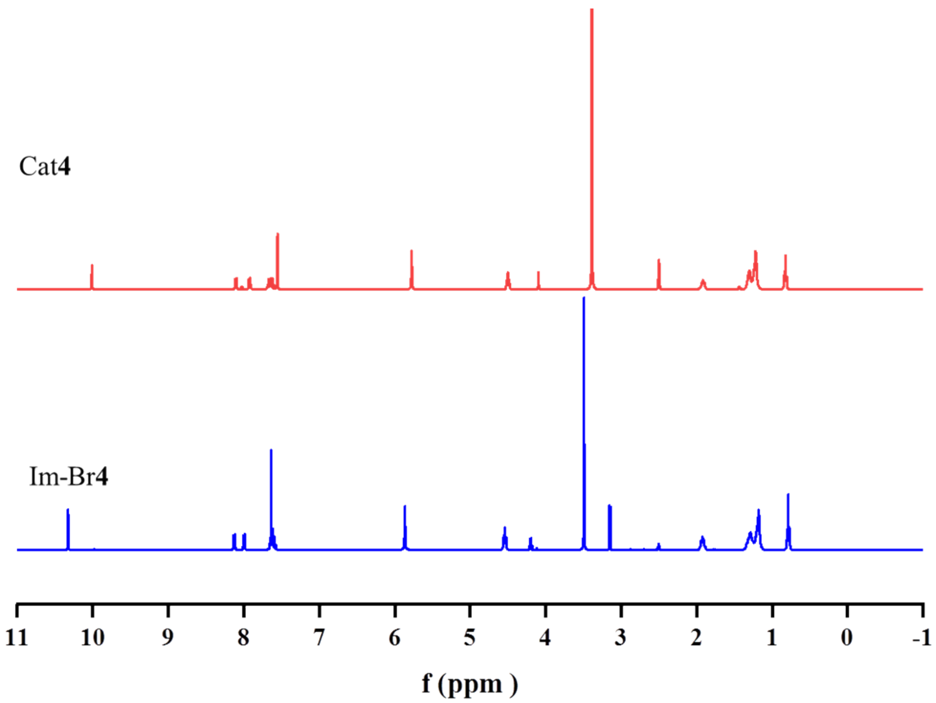

Fig. S7 [1]H NMR of Cat**4**/Im-Br**4** in DMSO-d_6.

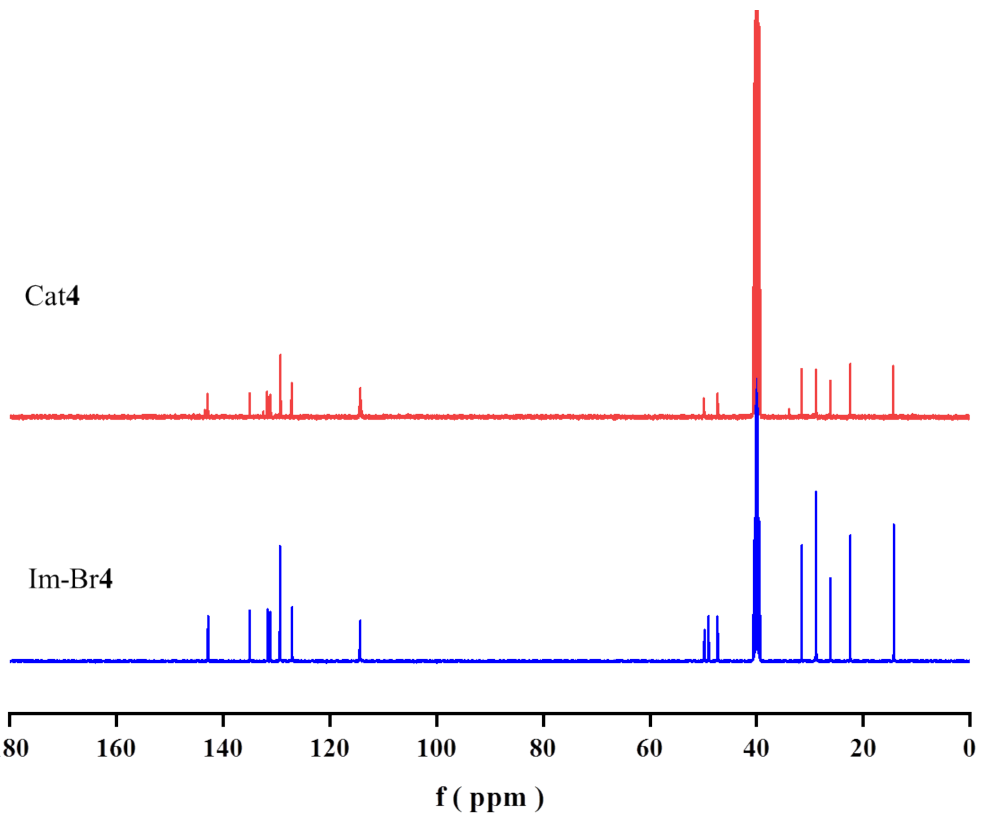

Fig. S8 [13]C NMR of Cat**4**/Im-Br**4** in DMSO-d_6.

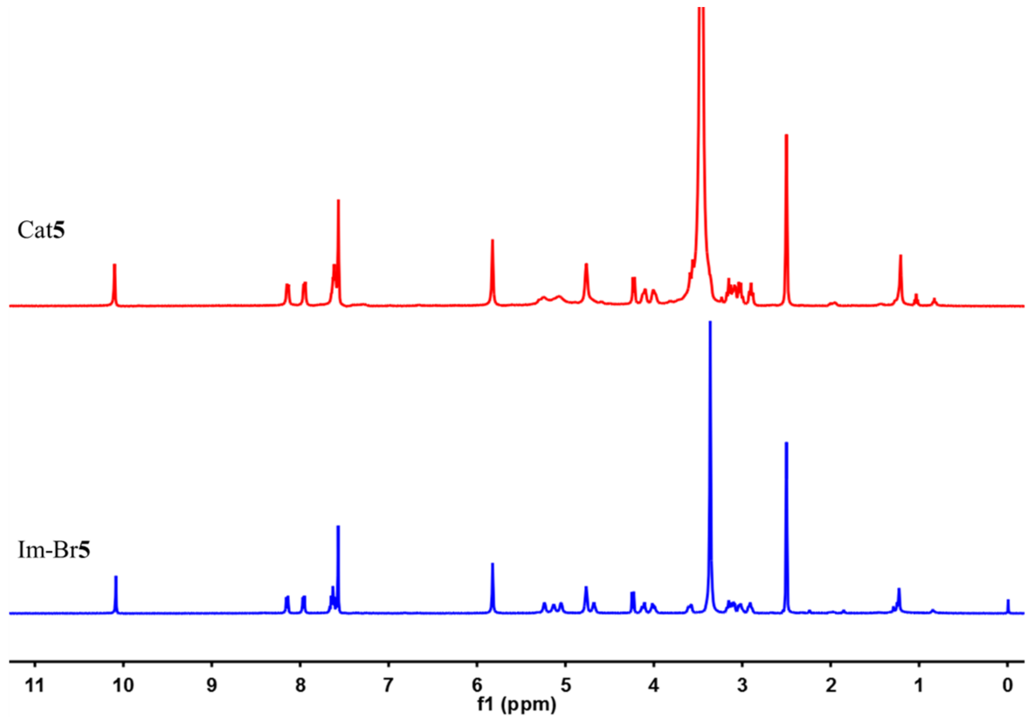

Fig. S9 ^{1}H NMR of Cat**5**/Im-Br**5** in DMSO-d_6.

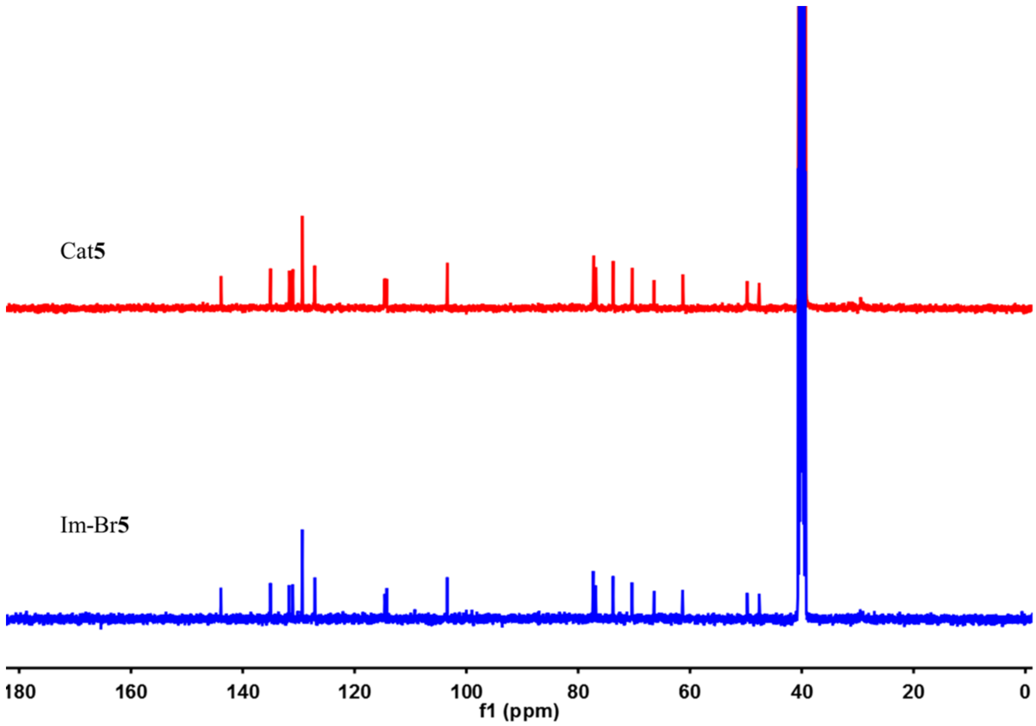

Fig. S10 ^{13}C NMR of Cat**5**/Im-Br**5** in DMSO-d_6.

3.2 Comparative FT-IR Spectra of Imidazolium Salts

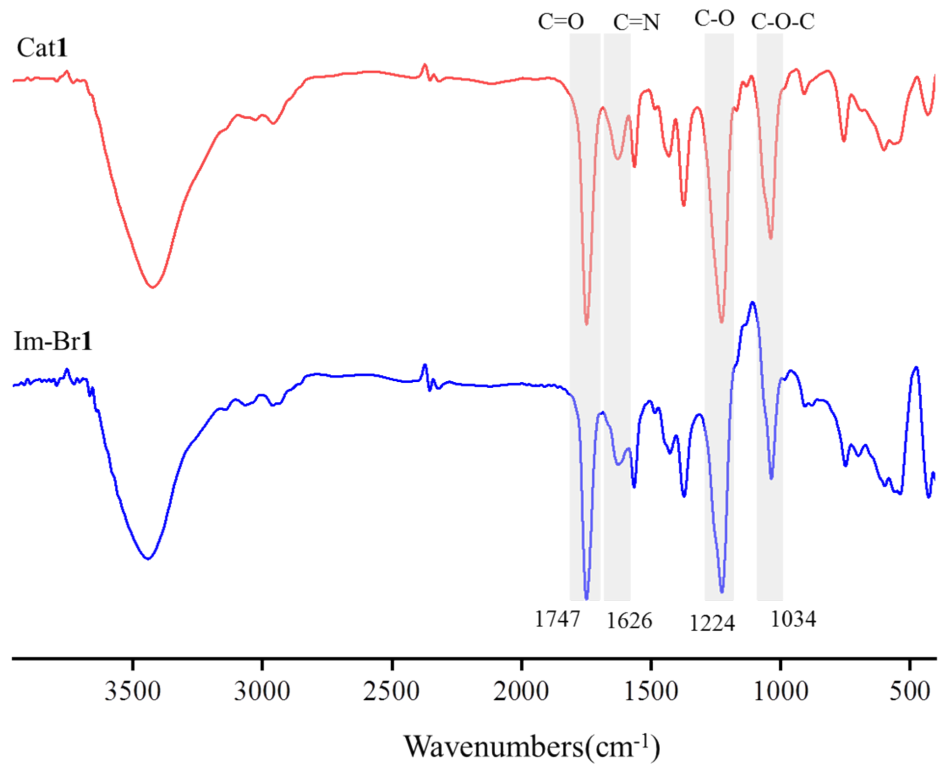

Fig. S11 FT-IR of Cat**1**/Im-Br**1**.

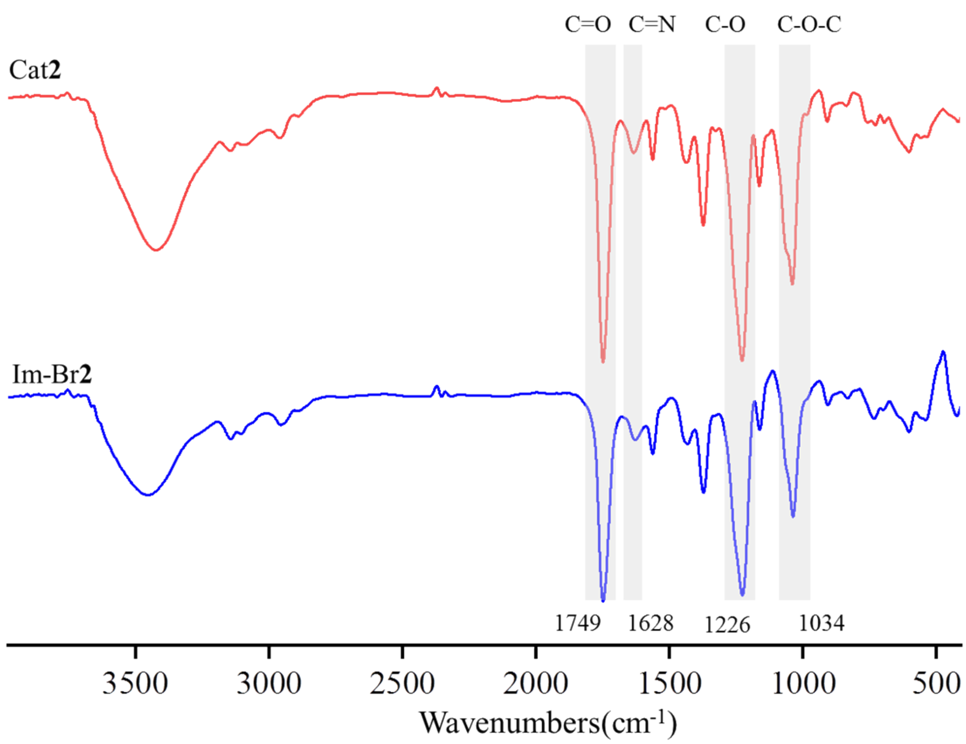

Fig. S12 FT-IR of Cat**2**/Im-Br**2**.

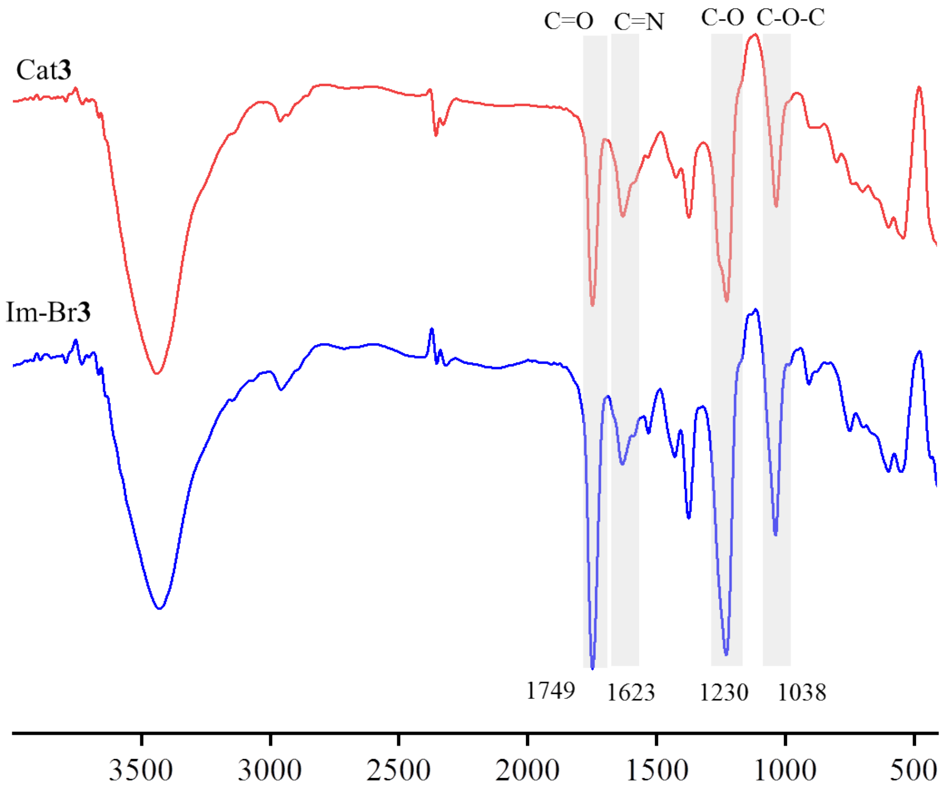

Fig. S13 FT-IR of Cat**3**/Im-Br**3**.

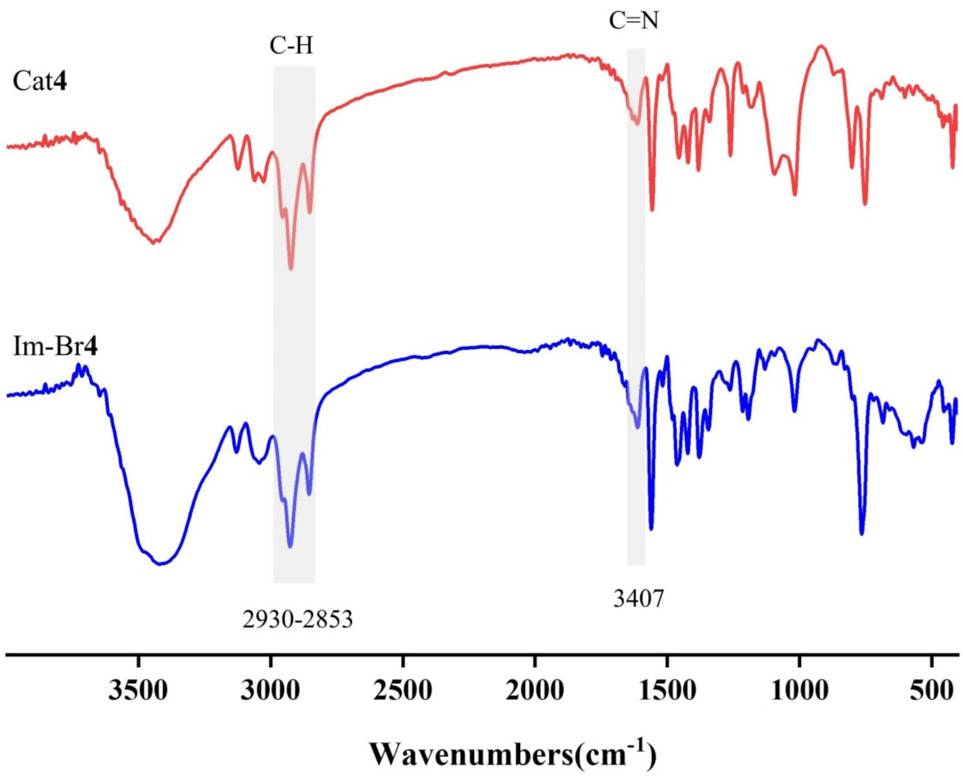

Fig. S14 FT-IR of Cat**4**/Im-Br**4**.

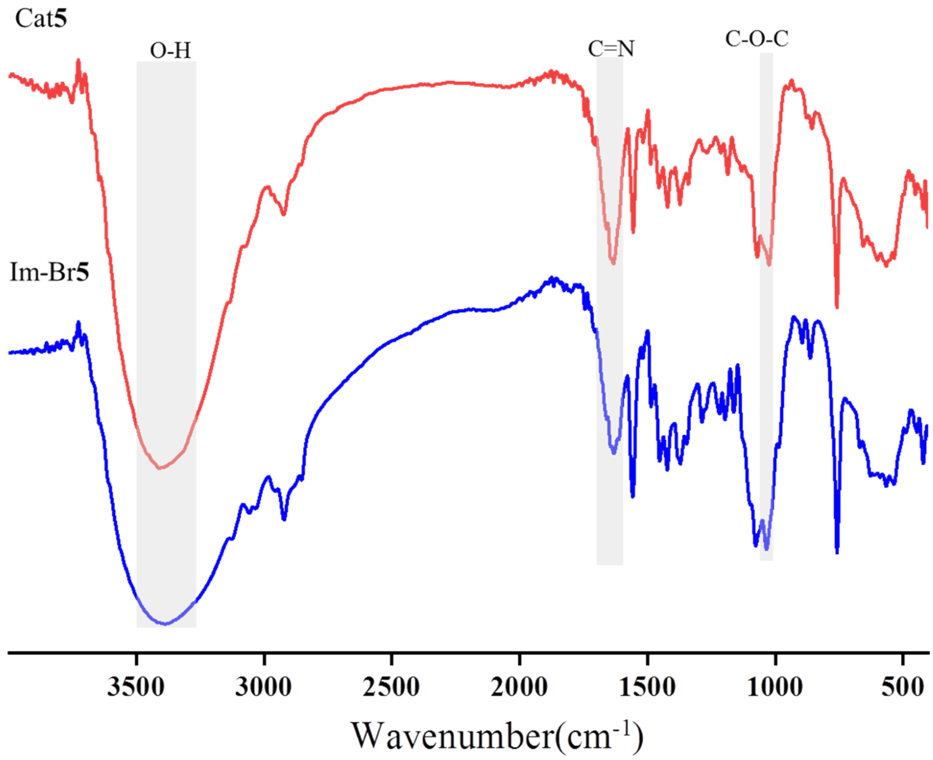

Fig. S15 FT-IR of Cat**5**/Im-Br**5**.

3.3 HR-MS Spectra of Imidazolium Salts

Formula Predictor Report **Printed at 2023/9/27 10:27:08**

Formula Predictor Result	**C54 H64 N4 O20**
Mass	544.20352
Error Margin	20 ppm
DBE Range	Not Used
Electron Ions	Both configurations
HC Ratio	Not Used
Nitrogen Rule	Not Used

Score	Pred. (M)	Pred. m/z	Meas. m/z	Diff. (mDa)	Formulae (M)	Ion	Diff. (ppm)	Iso Score	DBE
23.74	1088.41139	544.20515	544.20352	-1.63	C54 H64 N4 O20	[M]2+	-2.995	17.41	25.0

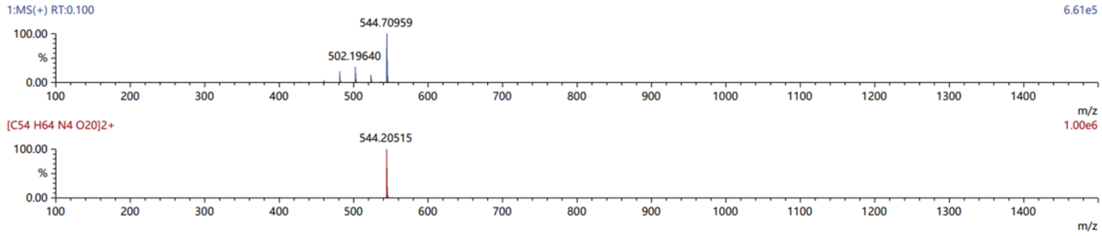

Fig. S16 HR/LC-MS of Im-Br**1**.

Formula Predictor Report **Printed at 2023/9/27 10:34:31**

Formula Predictor Result	**C46 H60 N4 O20**
Mass	494.1895
Error Margin	20 ppm
DBE Range	Not Used
Electron Ions	Both configurations
HC Ratio	Not Used
Nitrogen Rule	Not Used

Score	Pred. (M)	Pred. m/z	Meas. m/z	Diff. (mDa)	Formulae (M)	Ion	Diff. (ppm)	Iso Score	DBE
100.00	988.38009	494.18950	494.18950	0.00	C46 H60 N4 O20	[M]2+	0.000	100.00	19.0

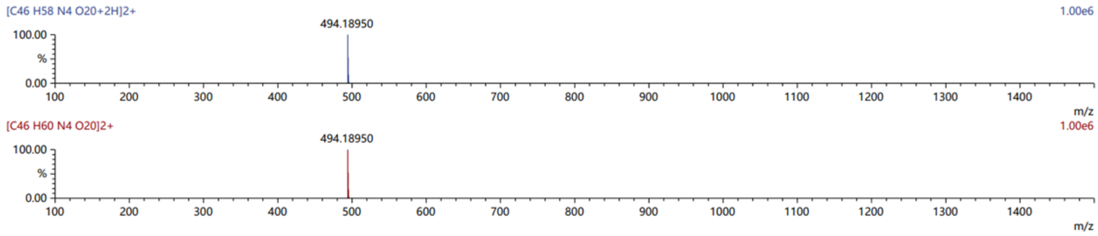

Fig. S17 HR/LC-MS of Im-Br**2**.

Formula Predictor Report **Printed at 2023/9/27 9:40:56**

Formula Predictor Result	**C48 H64 N4 O20**
Mass	508.20855
Error Margin	20 ppm
DBE Range	Not Used
Electron Ions	Both configurations
HC Ratio	Not Used
Nitrogen Rule	Not Used

Score	Pred. (M)	Pred. m/z	Meas. m/z	Diff. (mDa)	Formulae (M)	Ion	Diff. (ppm)	Iso Score	DBE
10.69	1016.41139	508.20515	508.20855	3.40	C48 H64 N4 O20	[M]2+	6.690	11.87	19.0

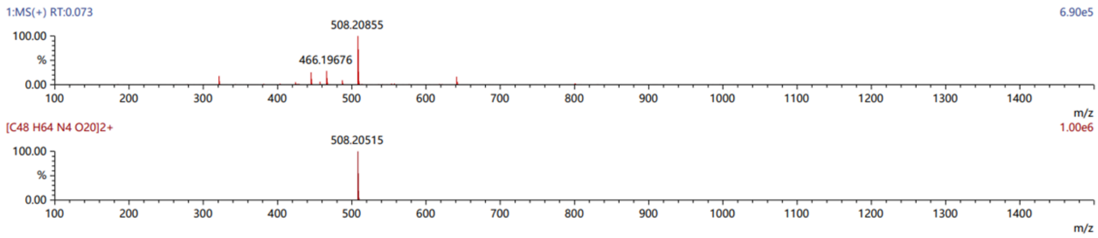

Fig. S18 HR/LC-MS of Im-Br**3**.

Formula Predictor Report — Printed at 2022/11/9 10:42:39

Formula Predictor Result	**C38 H52 N4**
Mass	282.21105
Error Margin	10 ppm
DBE Range	Not Used
Electron Ions	Both configurations
HC Ratio	Not Used
Nitrogen Rule	Not Used

#	Score	Pred. (M)	Pred. m/z	Meas. m/z	Diff. (mDa)	Formulae (M)	Ion	Diff. (ppm)	Iso Score	DBE
6	38.58	564.41920	282.20905	282.21105	2.00	C38 H52 N4	[M]2+	7.087	42.87	15.0

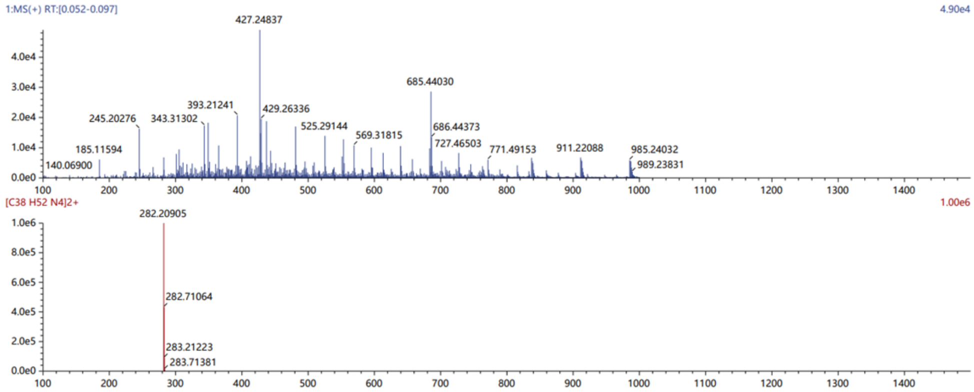

Fig. S19 HR/LC-MS of Im-Br**4**.

Formula Predictor Report — Printed at 2023/9/27 10:11:21

Formula Predictor Result	**C38 H48 N4 O12**
Mass	376.16494
Error Margin	20 ppm
DBE Range	Not Used
Electron Ions	Both configurations
HC Ratio	Not Used
Nitrogen Rule	Not Used

Score	Pred. (M)	Pred. m/z	Meas. m/z	Diff. (mDa)	Formulae (M)	Ion	Diff. (ppm)	Iso Score	DBE
34.90	752.32687	376.16289	376.16494	2.05	C38 H48 N4 O12	[M]2+	5.450	38.77	17.0

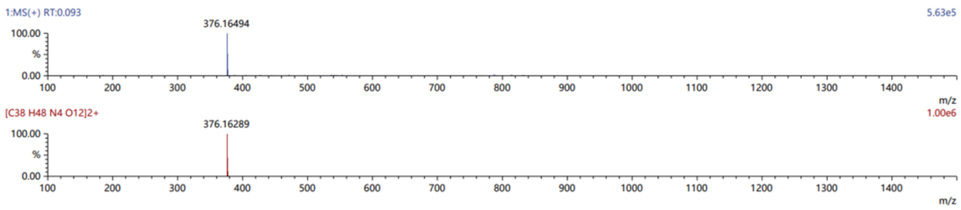

Fig. S20 HR/LC-MS of Im-Br**5**.

Formula Predictor Report — Printed at 2022/10/13 18:14:42

Formula Predictor Result	**C54 H64 N4 O20**
Mass	544.20901
Error Margin	10 ppm
DBE Range	Not Used
Electron Ions	Both configurations
HC Ratio	Not Used
Nitrogen Rule	Not Used

#	Score	Pred. (M)	Pred. m/z	Meas. m/z	Diff. (mDa)	Formulae (M)	Ion	Diff. (ppm)	Iso Score	DBE
1	40.00	1088.41139	544.20515	544.20901	3.86	C54 H64 N4 O20	[M]2+	7.093	44.44	25.0

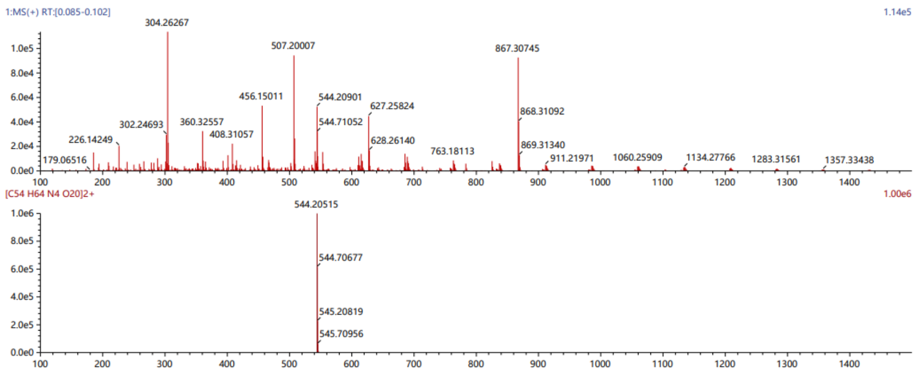

Fig. S21 HR/LC-MS of Cat**1**.

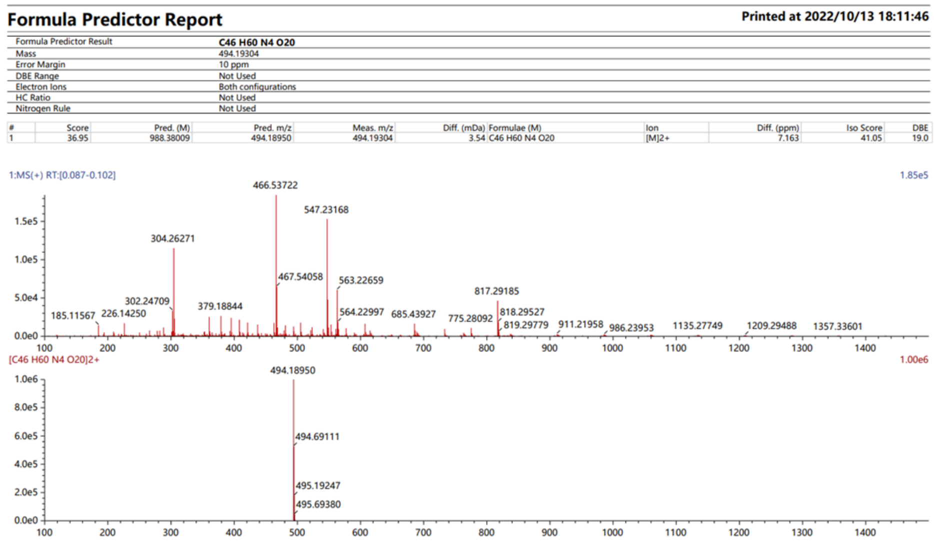

Fig. S22 HR/LC-MS of Cat**2**.

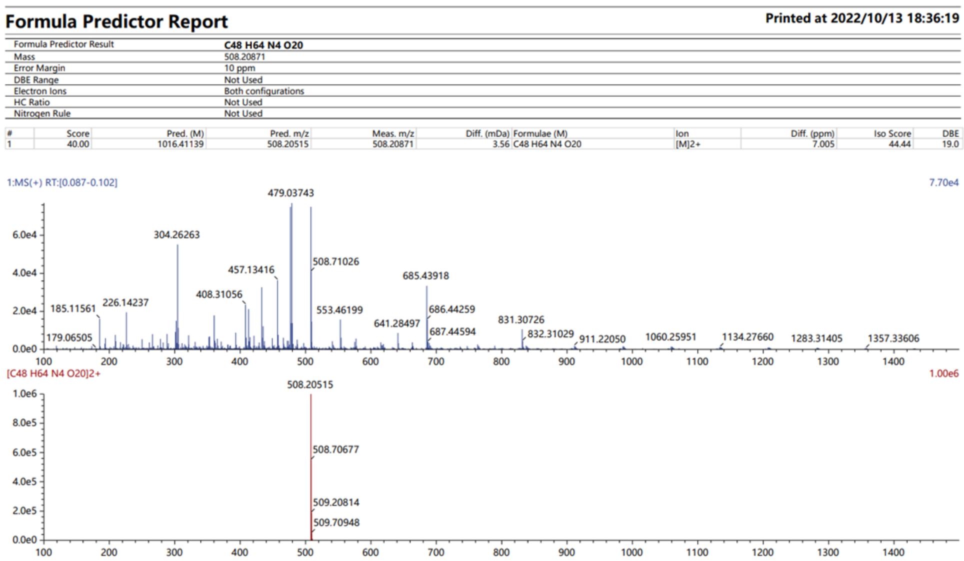

Fig. S23 HR/LC-MS of Cat**3**.

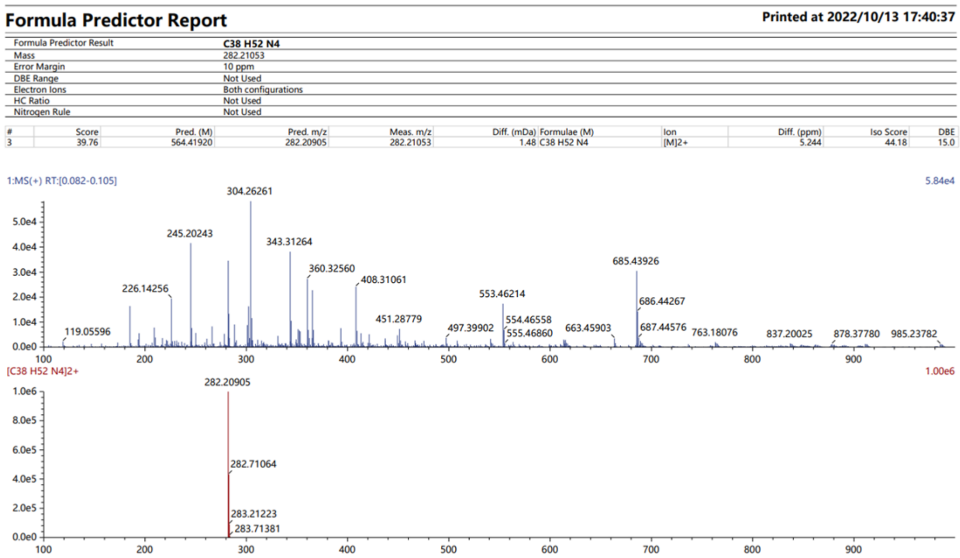

Fig. S24 HR/LC-MS of Cat**4**.

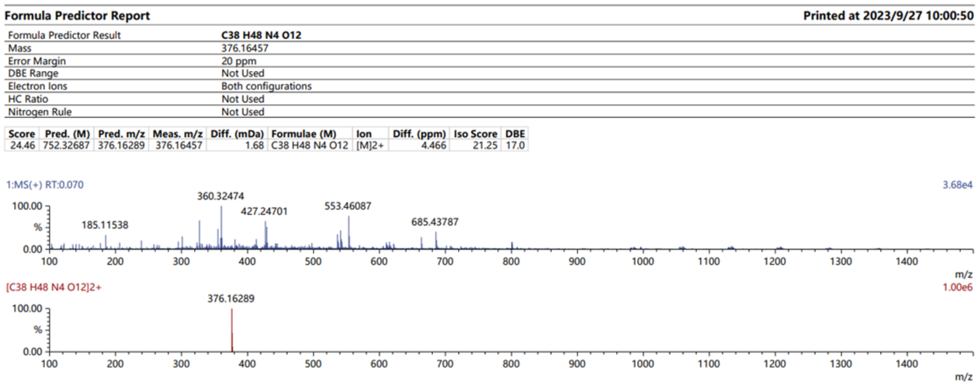

Fig. S25 HR/LC-MS of Cat**5**.

3.4 XPS Spectra of Cat1 and Cat5

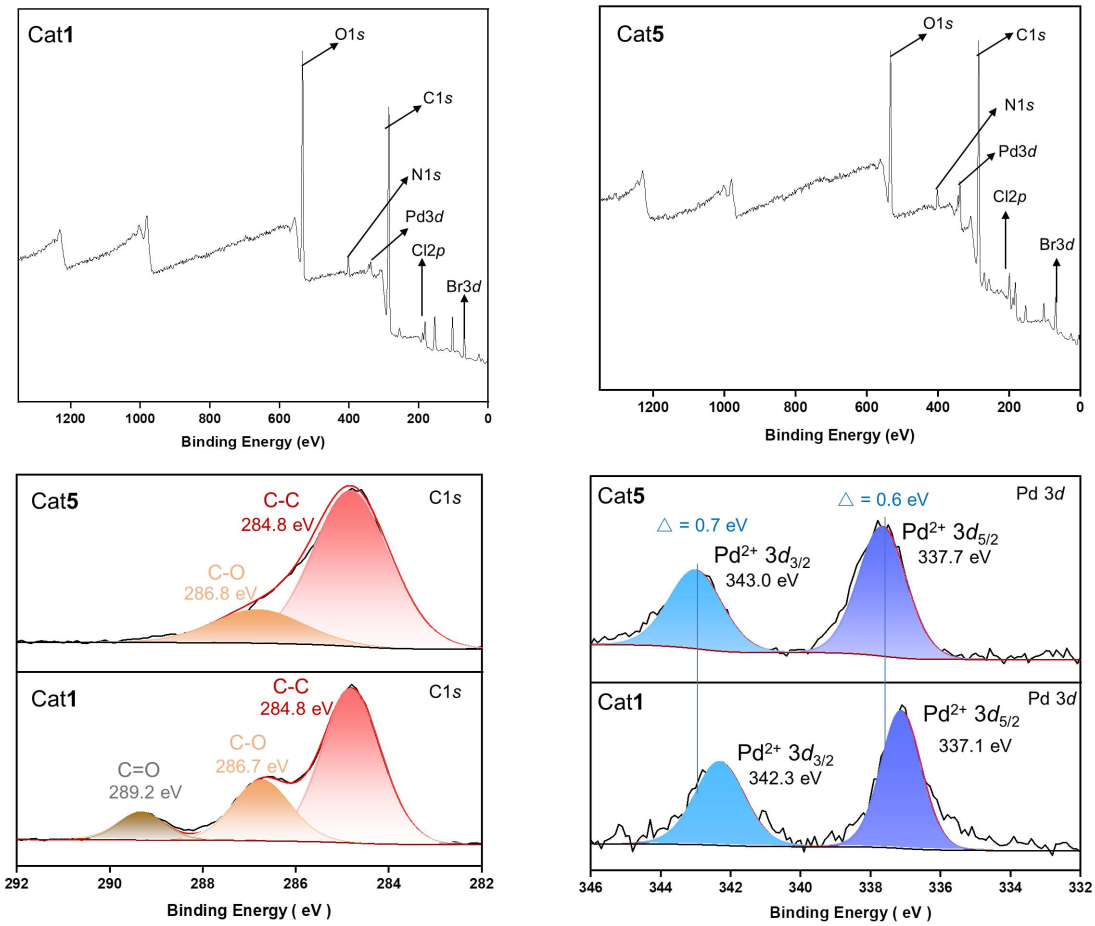

Fig. S26 XPS spectra of Cat**1** and Cat**5**.

3.5 TGA Spectra of Cat1-5

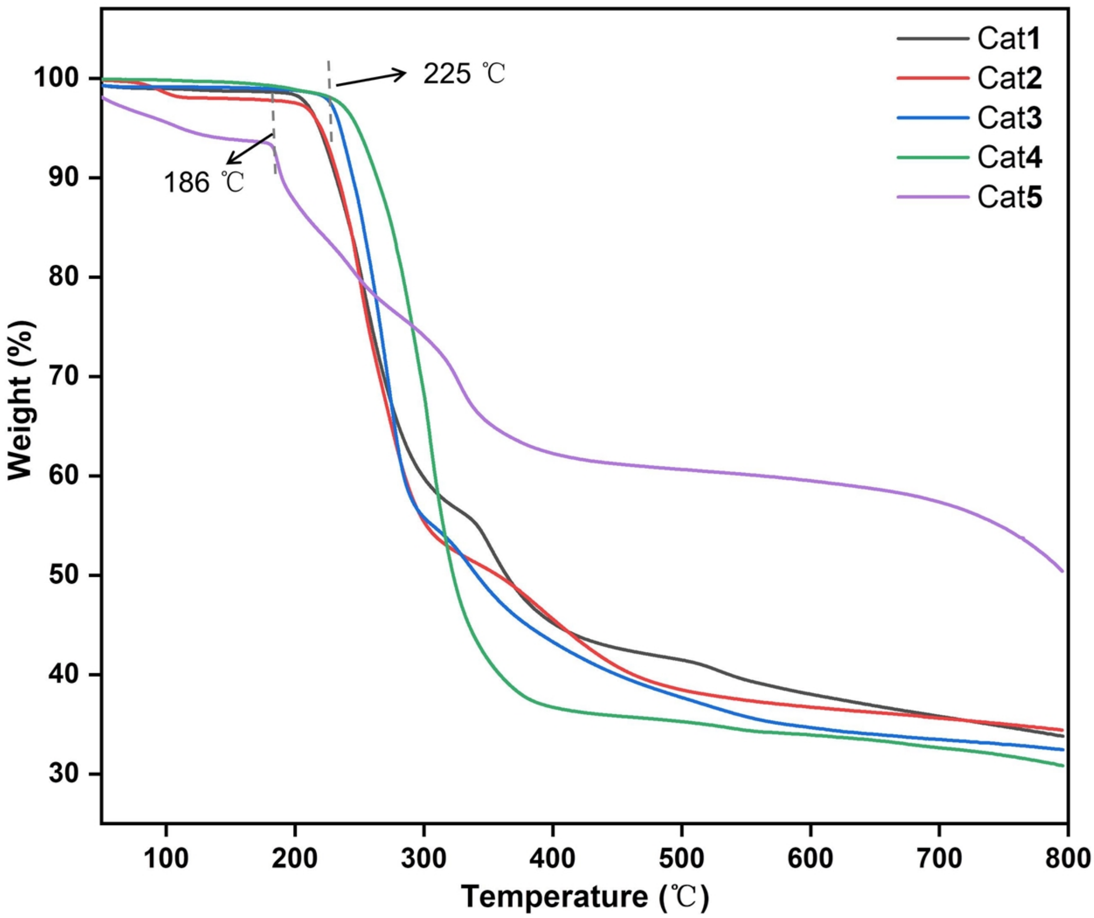

Fig. S27 TGA spectra of Cat**1-5.**

3.6 NMR Spectra and Color of Cat1 at Different Temperatures

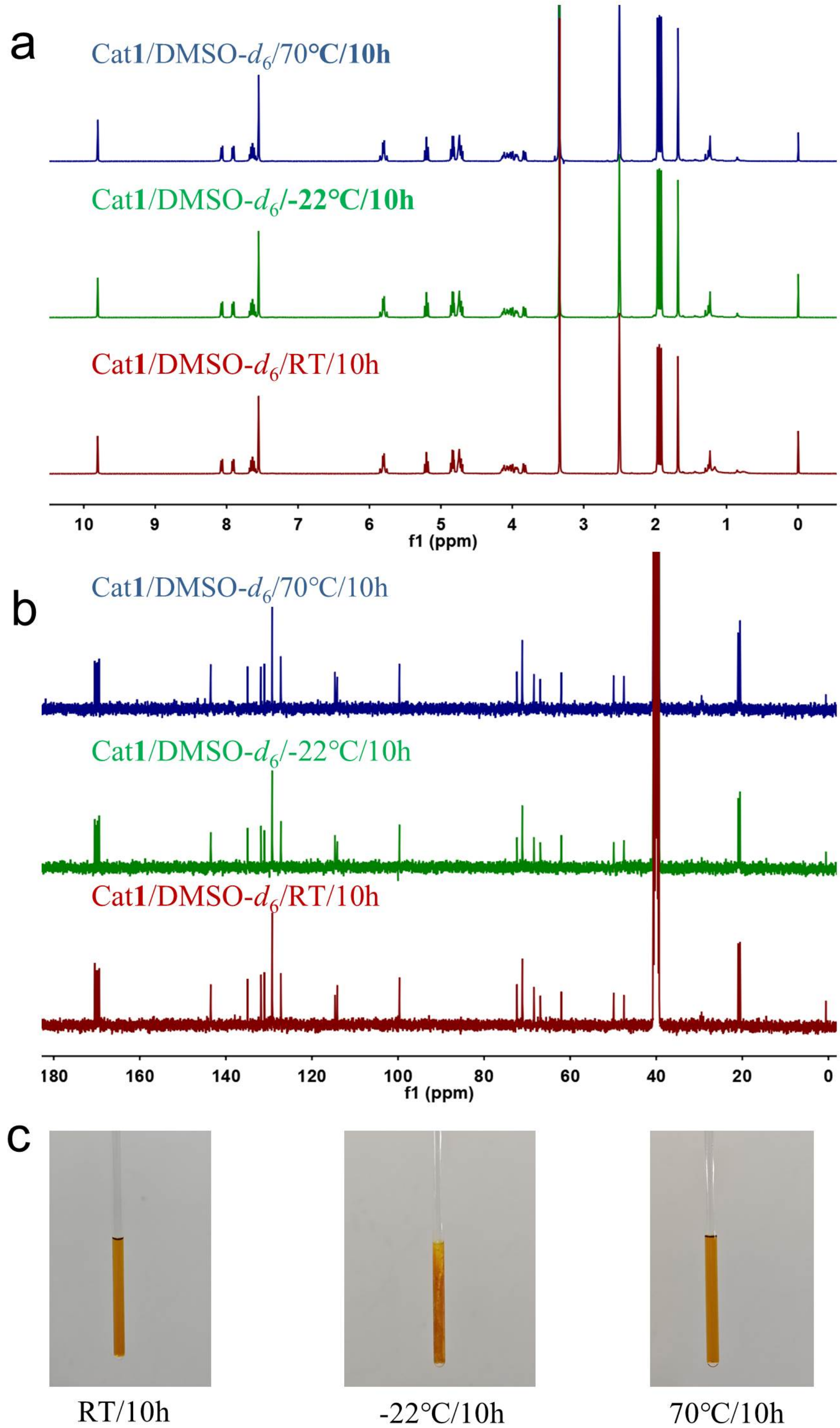

Fig. S28 NMR spectra (a and b) and color (c) of Cat**1** in DMSO-d_6 at -22℃, 25-30℃, and 70℃.

4. Kinetic Experiments

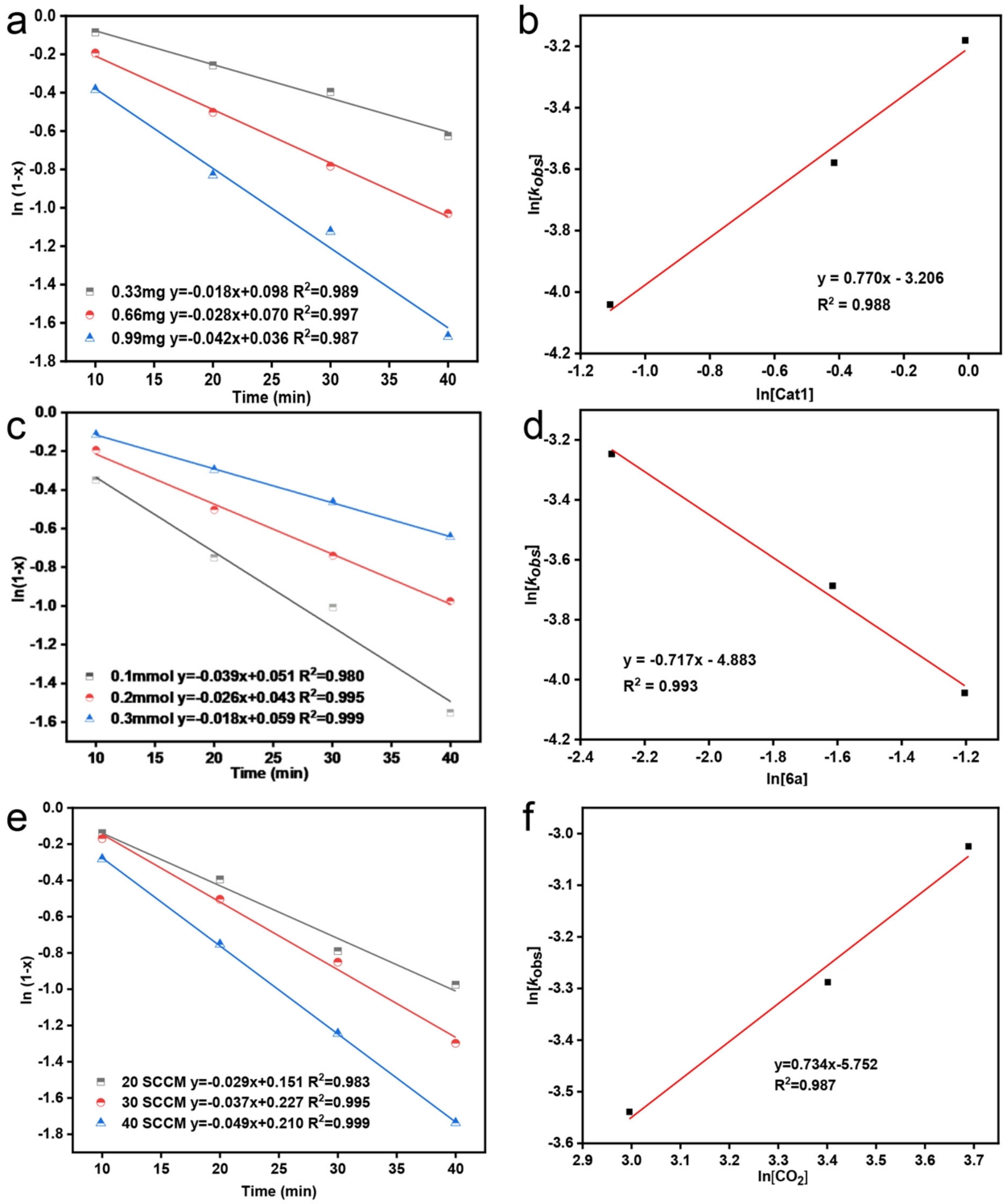

Fig. S29 a Pseudo-first order kinetic plots ($\ln(1\text{-x})$ versus time) of three different dosages of Cat**1**. b Curve fitting of $\ln[k_{obs}]$ against ln[Cat**1**]. c Pseudo-first order kinetic plots $\ln(1\text{-x})$ versus time of three different concentrations of **6a**. d Curve fitting of $\ln[k_{obs}]$ against ln[**6a**]; e Pseudo-first order kinetic plots ($\ln(1\text{-x})$ versus time) of three different flow rates of CO_2. f curve fitting of $\ln[k_{obs}]$ against ln[CO_2].

5. Gram-scale Reaction, Product Properties, and 1H NMR Spectra

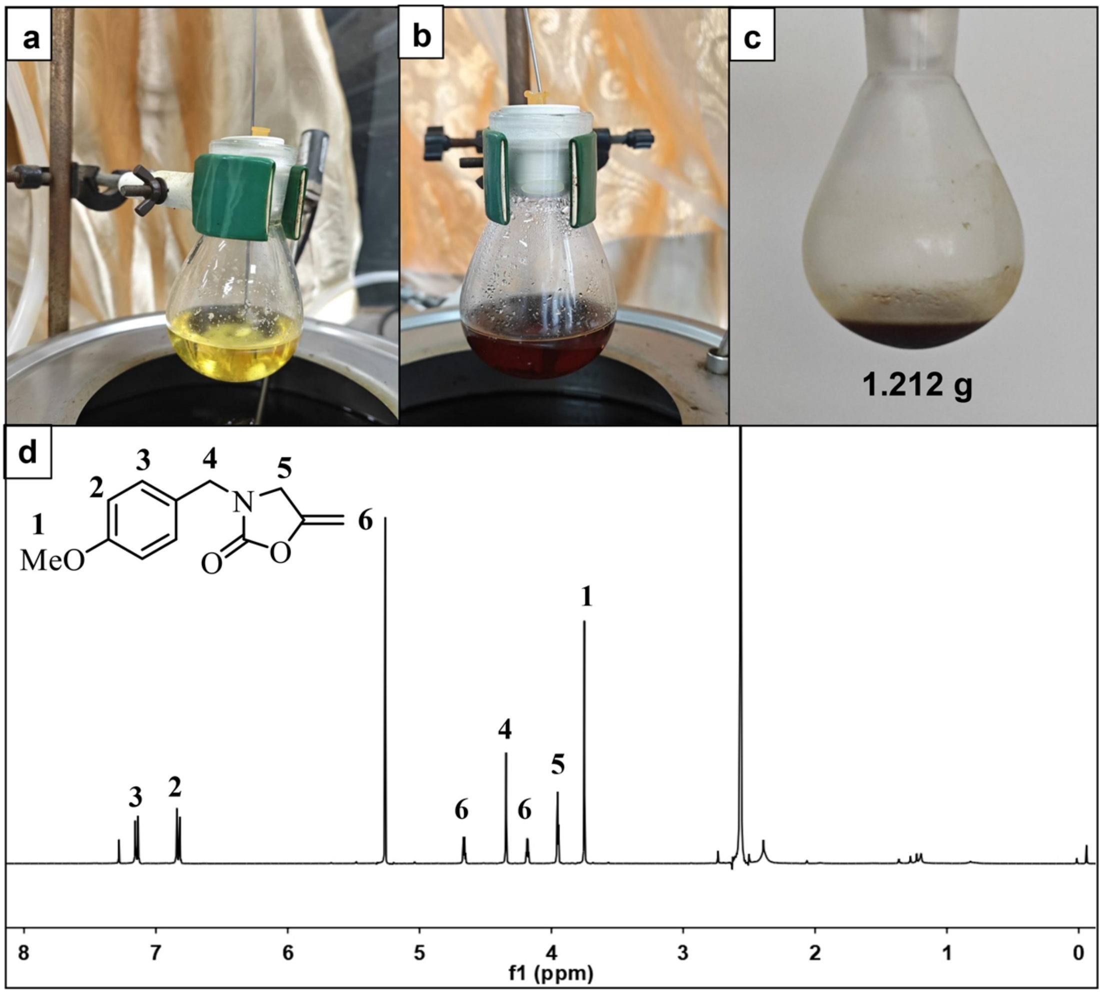

Fig. S30 Gram-scale synthesis. The reactions were carried out with **6a** (6.0 mmol, 1.05 g), Cat**1** (5.0 mol%, 6.6 mg), simulated flue gas (bubbling), NaOAc (3.0 mmol, 0.246 g), DMSO (20.0 mL) and stirred at 70 ^{o}C for 3.0 h. a System color before reaction; b System color after reaction. c Properties of purified product **7a**. d ^{1}H NMR of purified product **7a**.

6. Catalyst Stability Evaluation

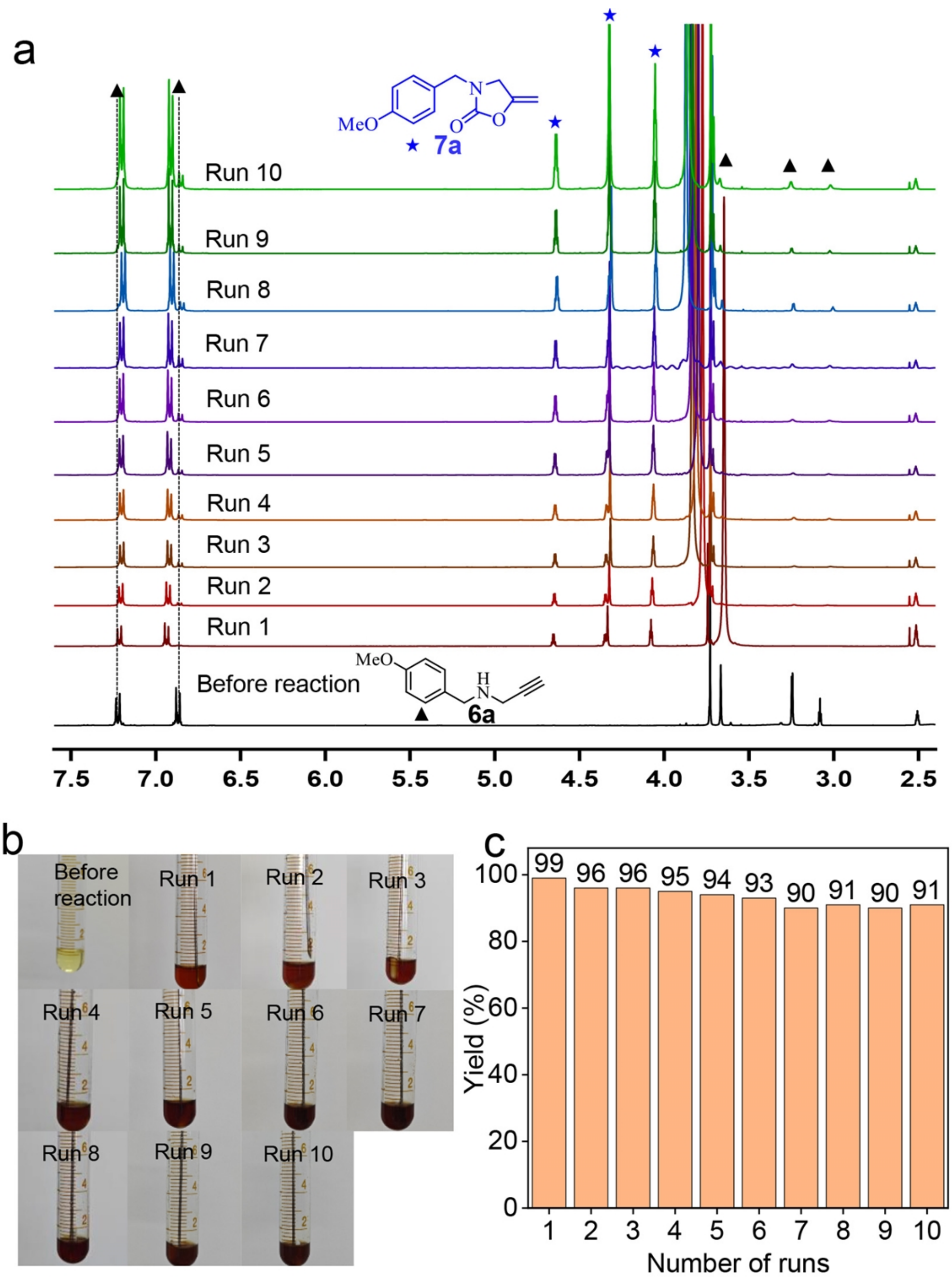

Fig. S31 The cycle catalytic performance of catalyst Cat**1**. Reaction conditions: **6a** (0.1 mmol, 17.5 mg), Cat**1** (0.5 mol%, 0.66 mg), simulated flue gas (bubbling), NaOAc (0.3 mmol, 24.6 mg), DMSO (1.0 mL) and stirred at 70^{o}C for 1.0 h. After each reaction, fresh **6a** was added to the catalytic system. Yields were determined by ^{1}H NMR. a Catalyst recycling study for Cat**1**. b Photos of catalytic system. c ^{1}H NMR tracked catalytic system.

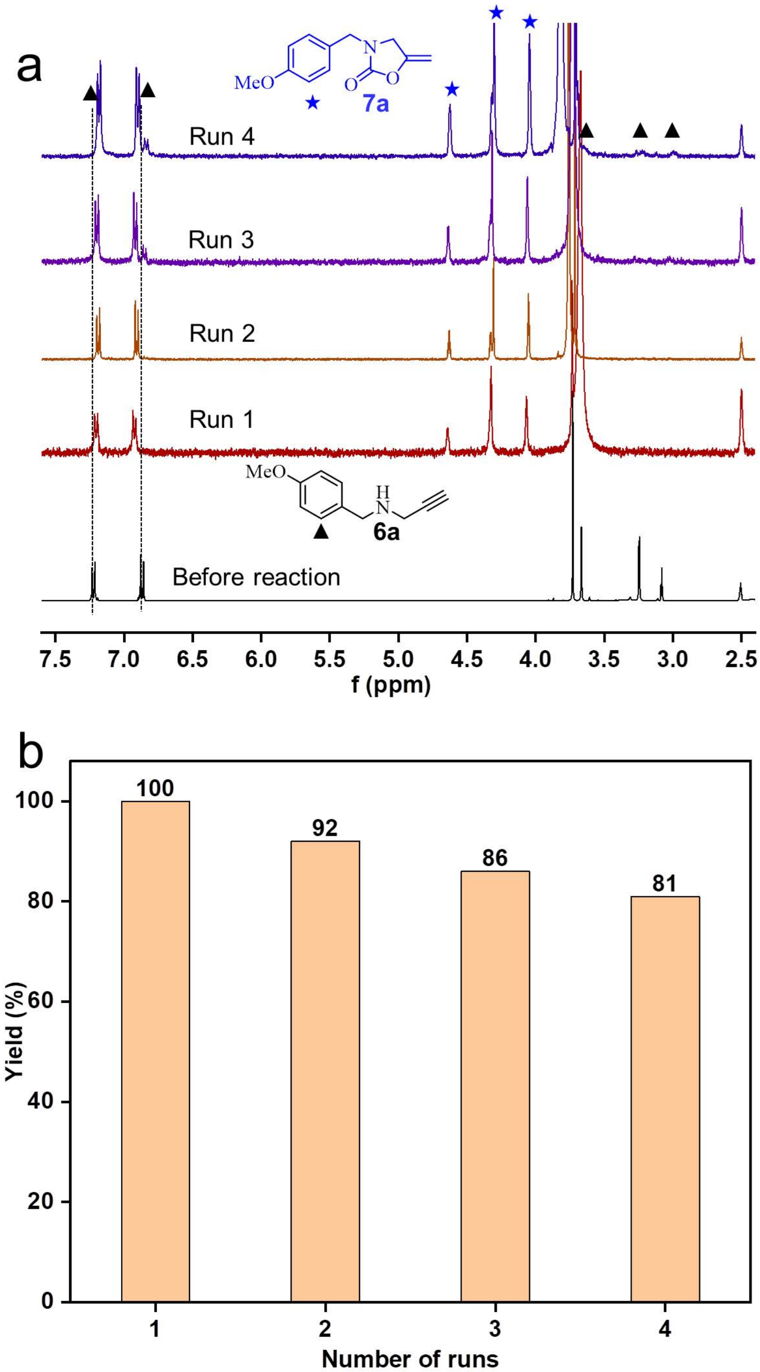

Fig. S32 The cycle catalytic performance of catalyst Cat**5**. Reaction conditions: **6a** (0.1 mmol, 17.5 mg), Cat**5** (0.75 mol%, 0.78 mg), simulated flue gas (bubbling), NaOAc (0.3 mmol, 24.6 mg), DMSO-d_6 (1.0 mL) and stirred at 70^{o}C for 1.0 h. After each reaction, fresh **6a** was added to the catalytic system. Yields were determined by ^{1}H NMR. a Catalyst recycling study for Cat**5**. b ^{1}H NMR tracked catalytic system.

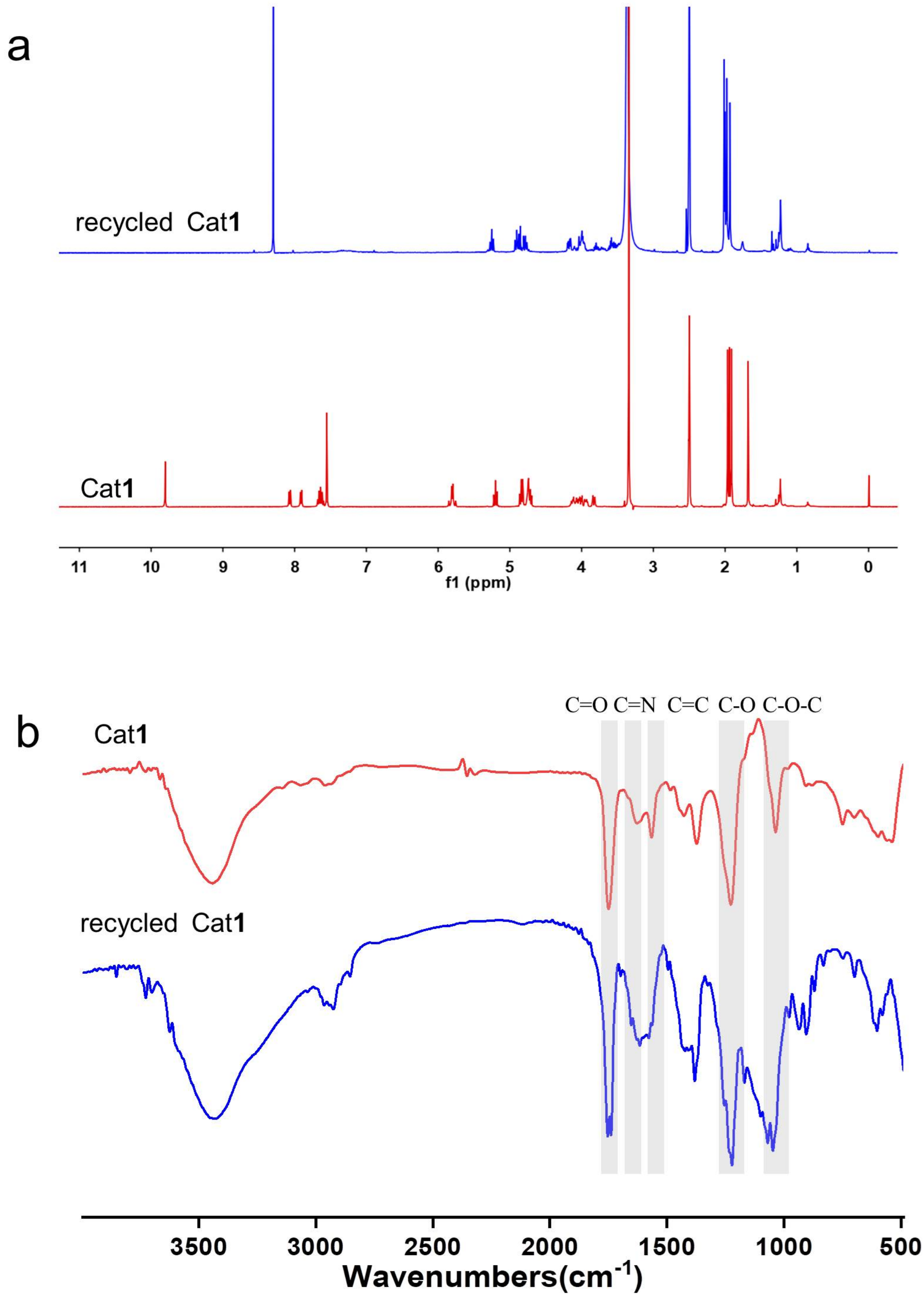

Fig. S33 a ^{1}H NMR spectra of Cat**1** and recycled Cat**1**. b FT-IR spectra of Cat**1** and recycled Cat**1**.

7. Mechanism Exploration

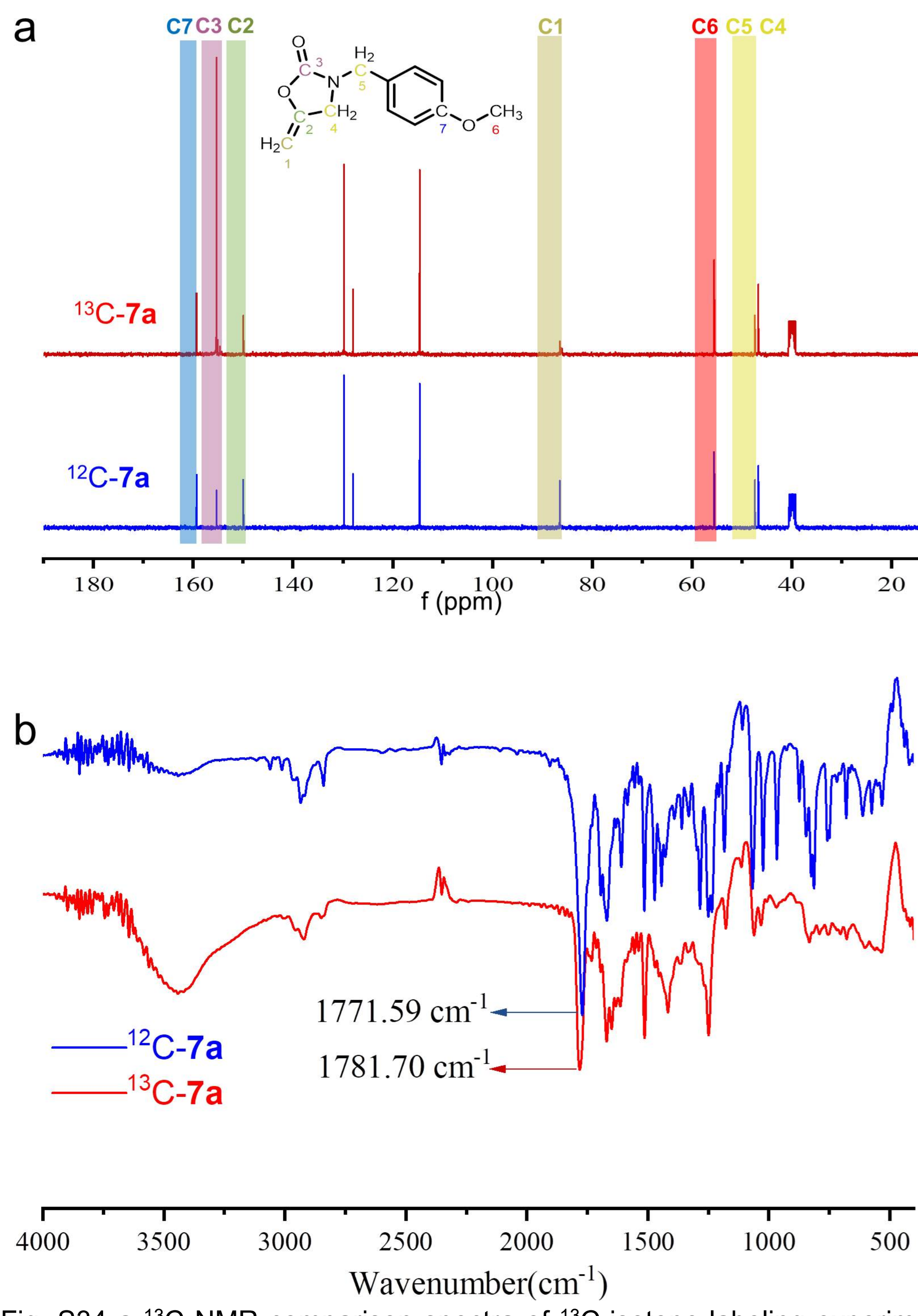

Fig. S34 a ^{13}C NMR comparison spectra of ^{13}C-isotope-labeling experiments for **7a**. b FT-IR spectra of ^{13}C-isotope-labeling experiments for **7a**.

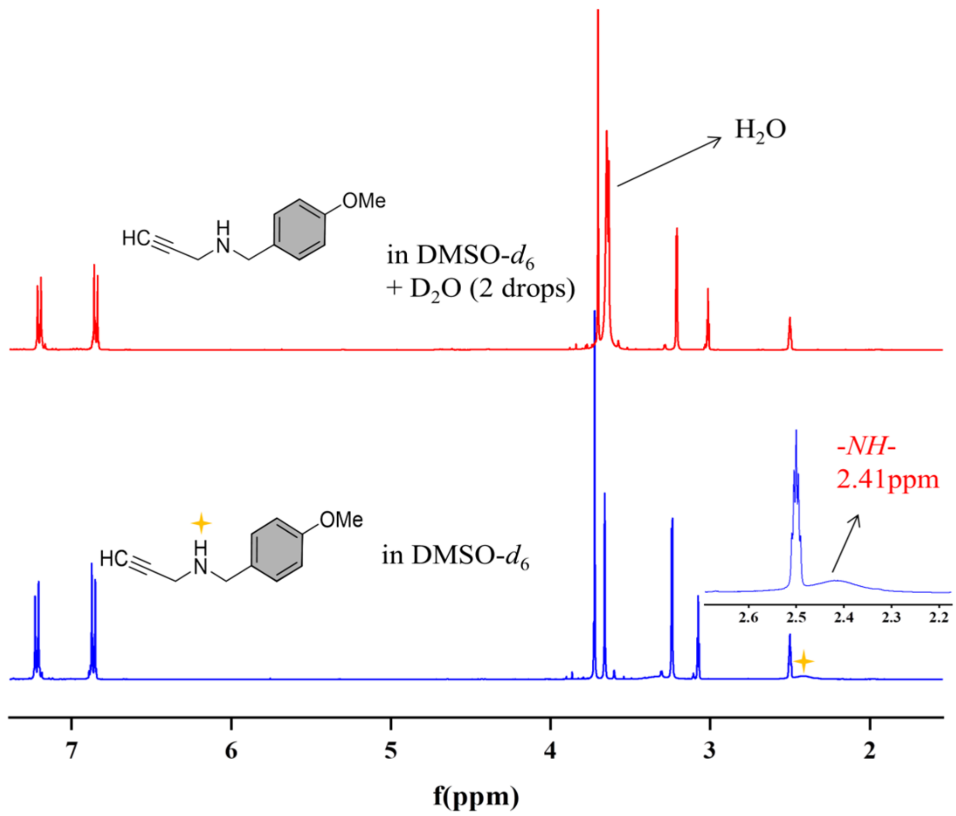

Fig. S35 Hydrogen–deuterium exchange experiment in D_2O/DMSO-d_6.

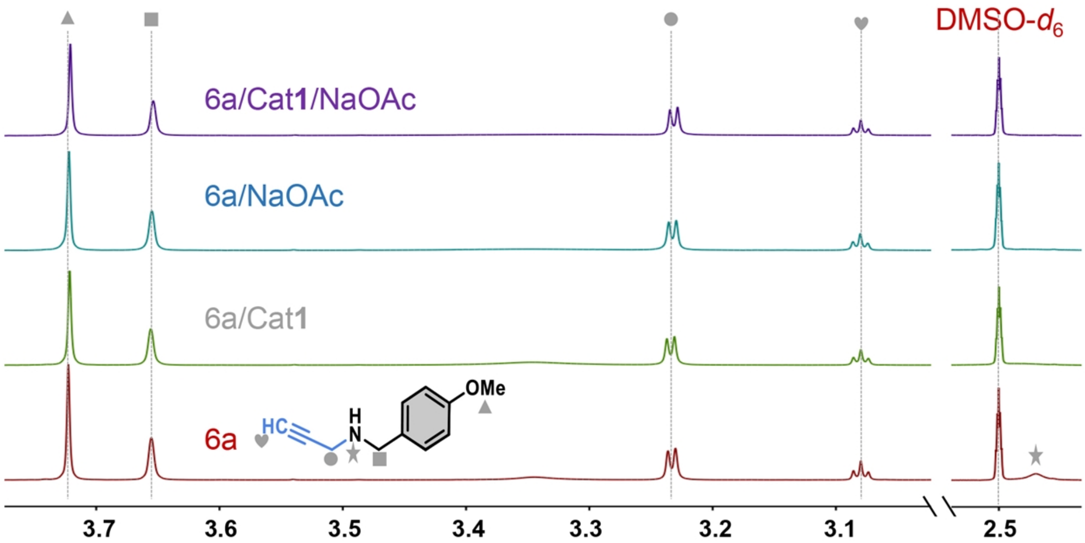

Fig. S36 Partially ^{1}H NMR spectra monitoring of substrate **6a**, **6a**/Cat**1**, **6a**/NaOAc, and **6a**/Cat**1**/NaOAc in DMSO-d_6.

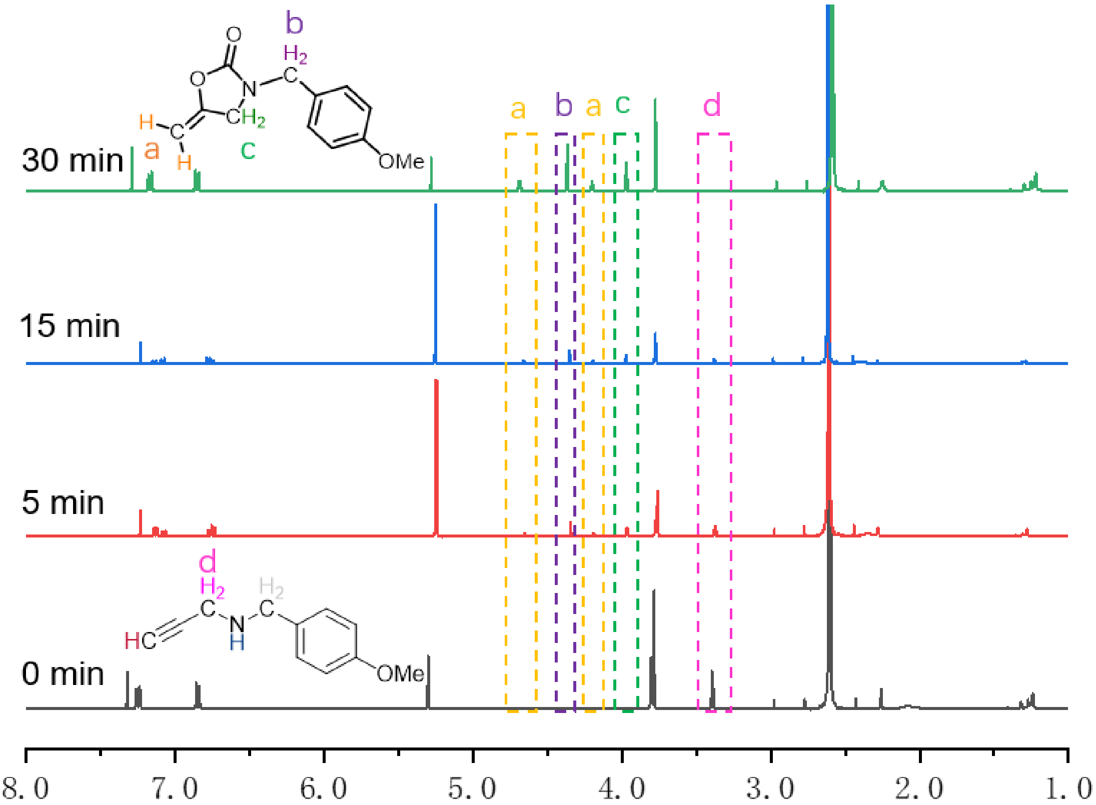

Fig. S37 Partially [1]H NMR spectra monitoring of Cat**1**-catalyzed carboxylative cyclization of **6a** and CO_2 at 70°C.

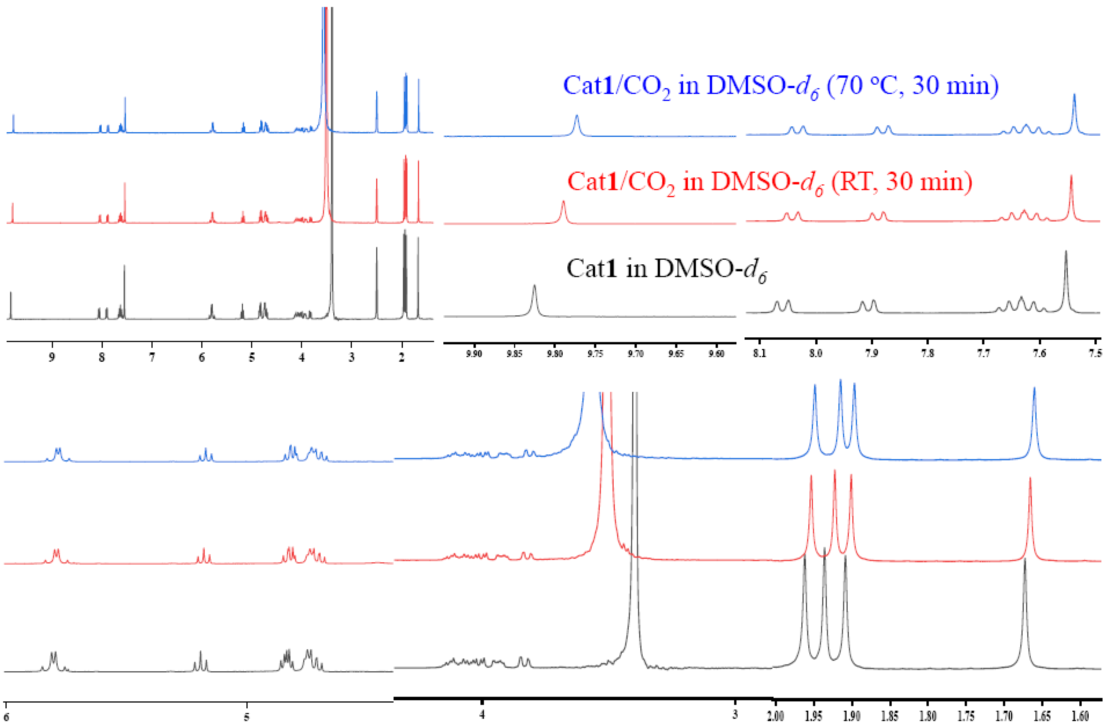

Fig. S38 The interactions between Cat**1** and CO_2 were investigated by [1]H NMR.

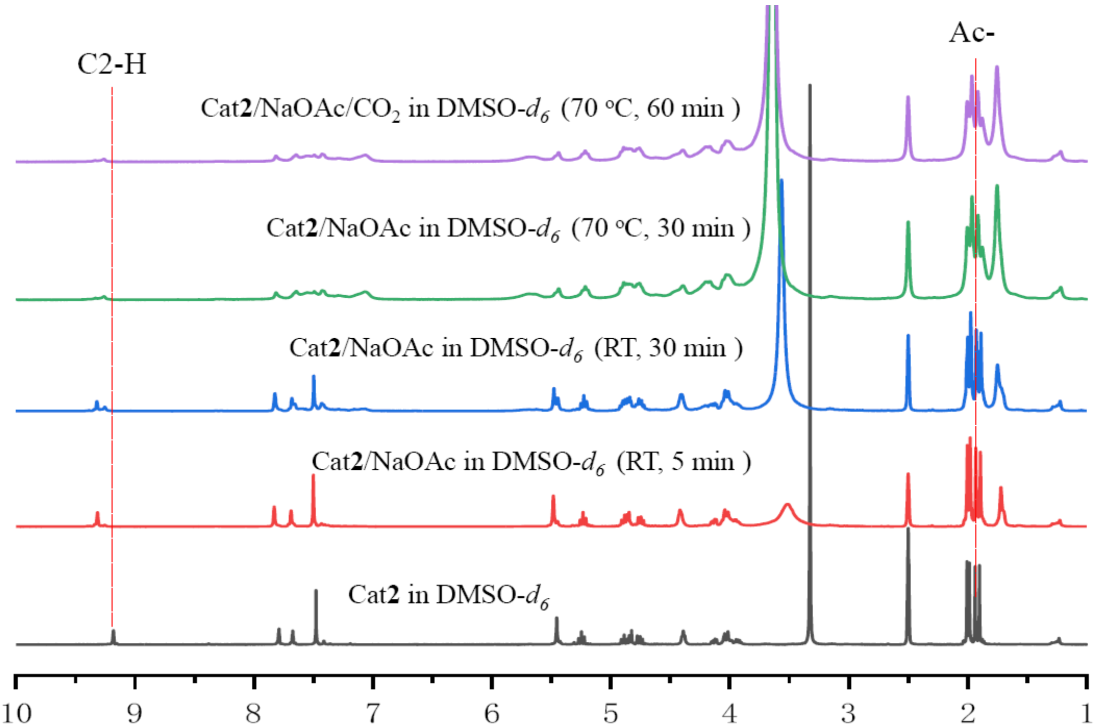

Fig. S39 The interactions between Cat**2** and NaOAc were investigated by [1]H NMR.

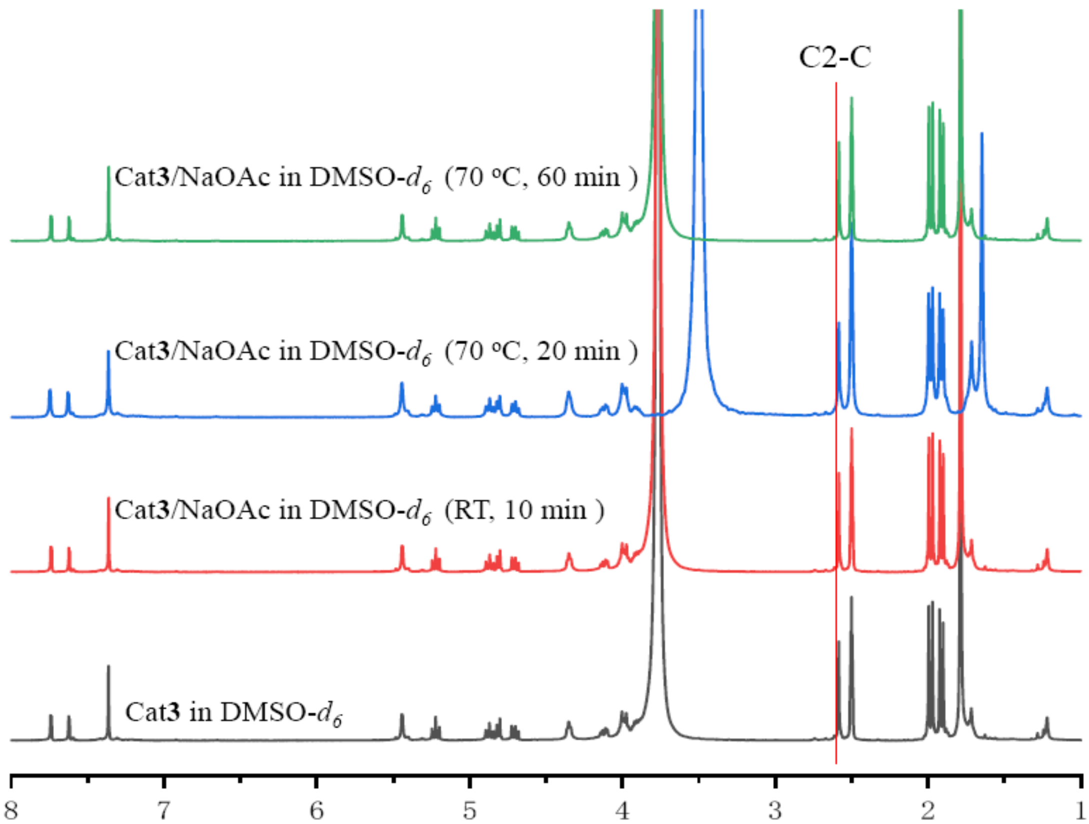

Fig. S40 The interactions between Cat**3** and NaOAc were investigated by [1]H NMR.

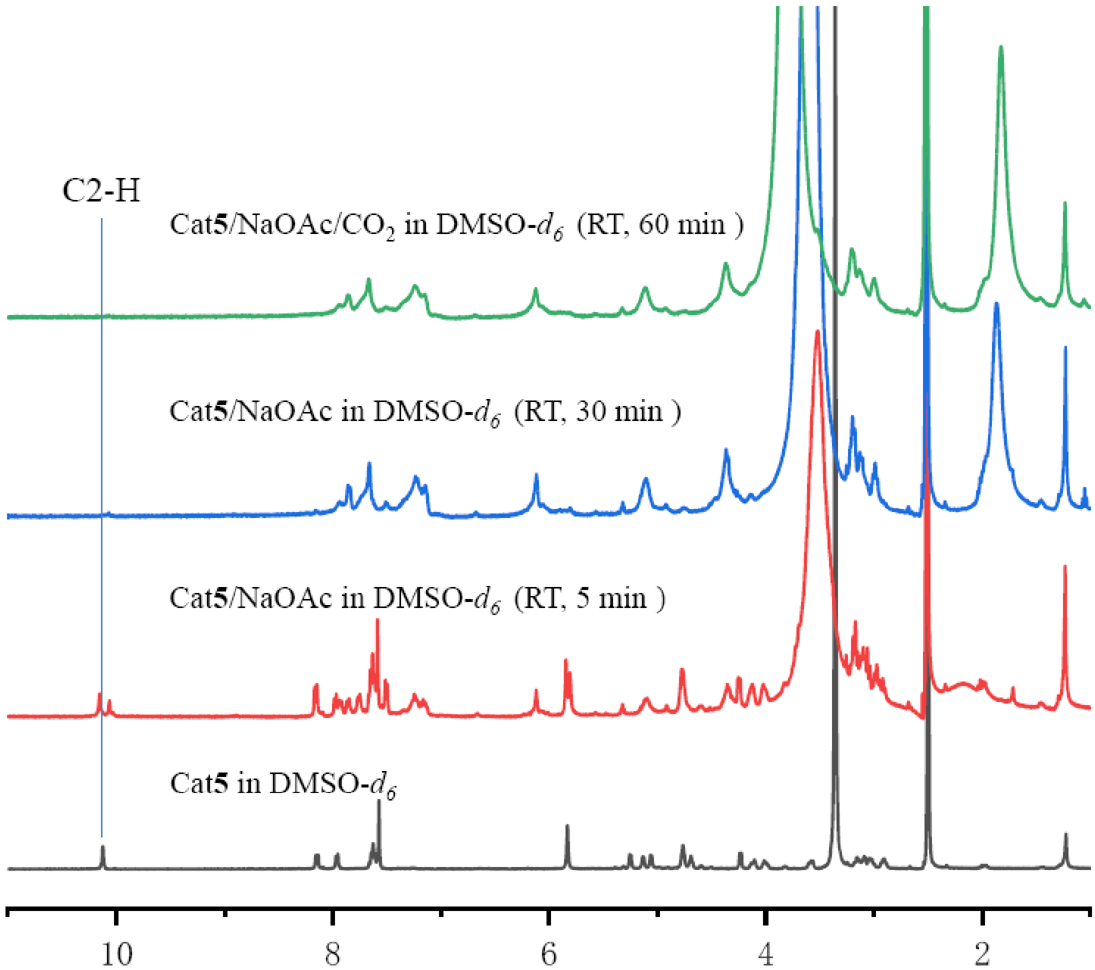

Fig. S41 The interactions between Cat**5**, NaOAc, and CO_2 were investigated by ^{1}H NMR.

7. NMR Spectra of Imidazolium Salts

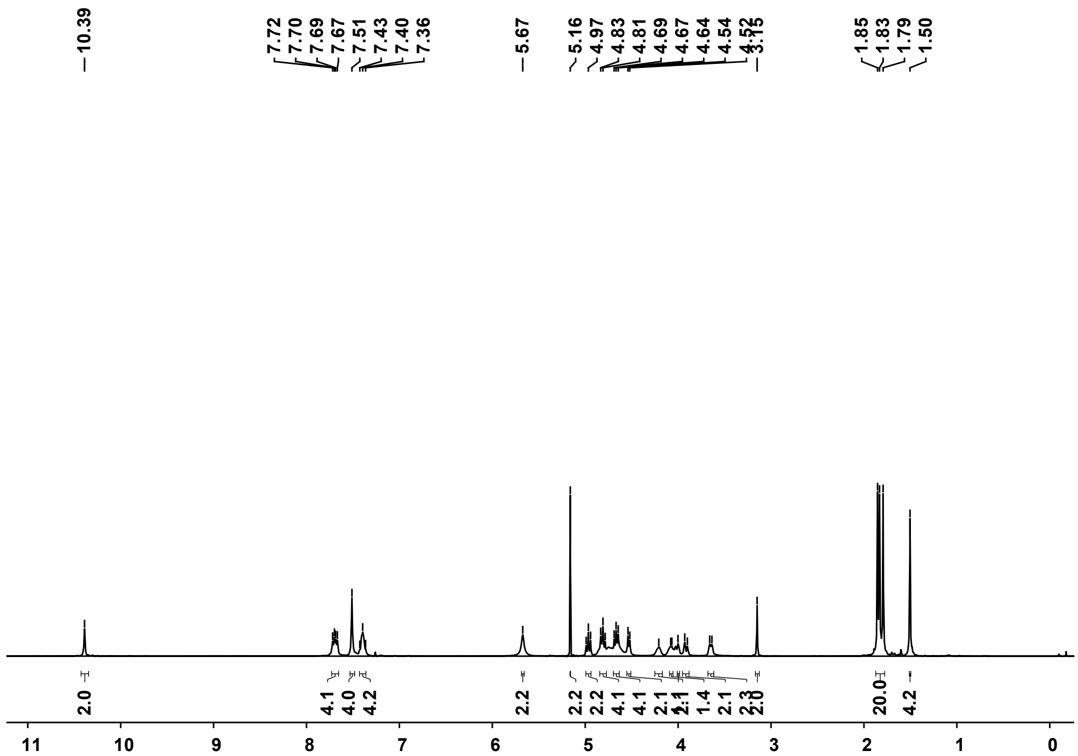

Fig. S42 ^{1}H NMR of Im-Br**1** in $CDCl_3$.

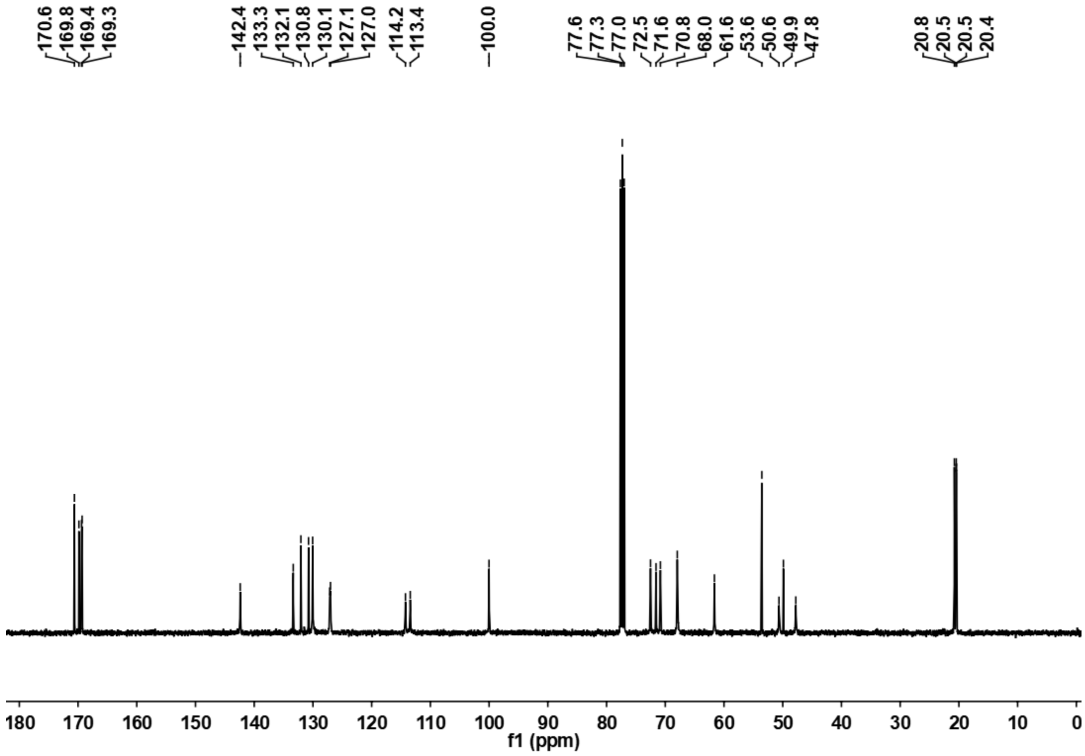

Fig. S43 ^{13}C NMR of Im-Br**1** in $CDCl_3$.

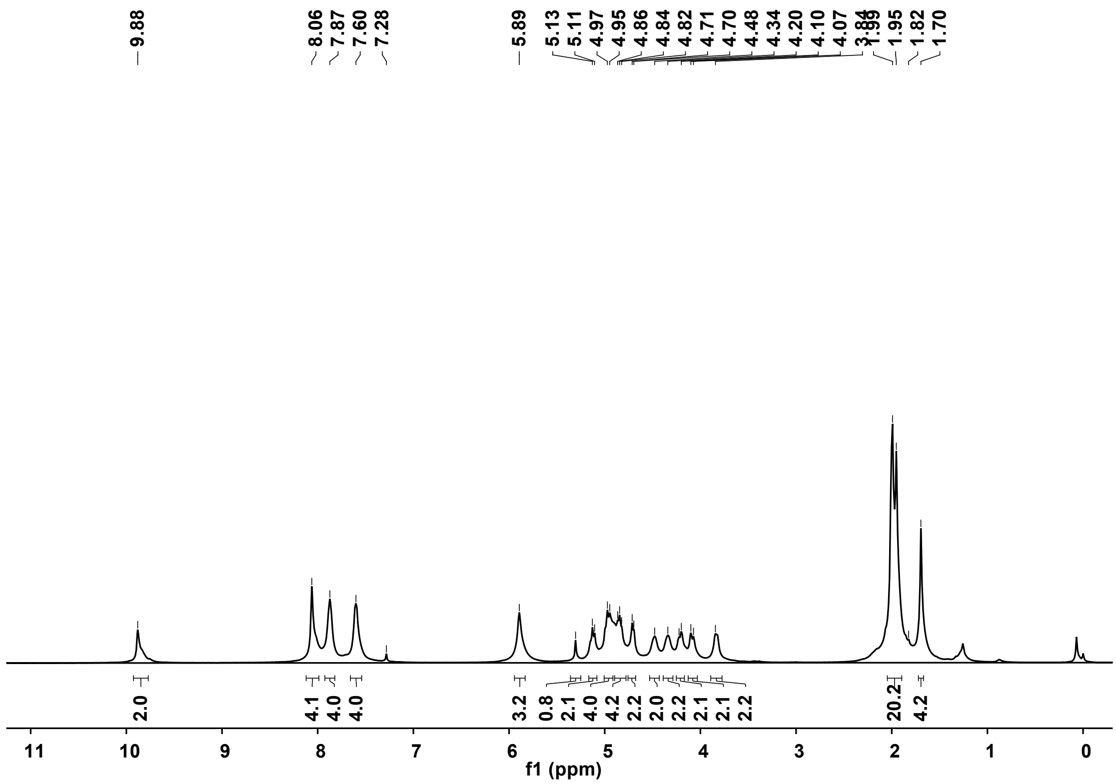

Fig. S44 ^{1}H NMR of Cat**1** in $CDCl_3$.

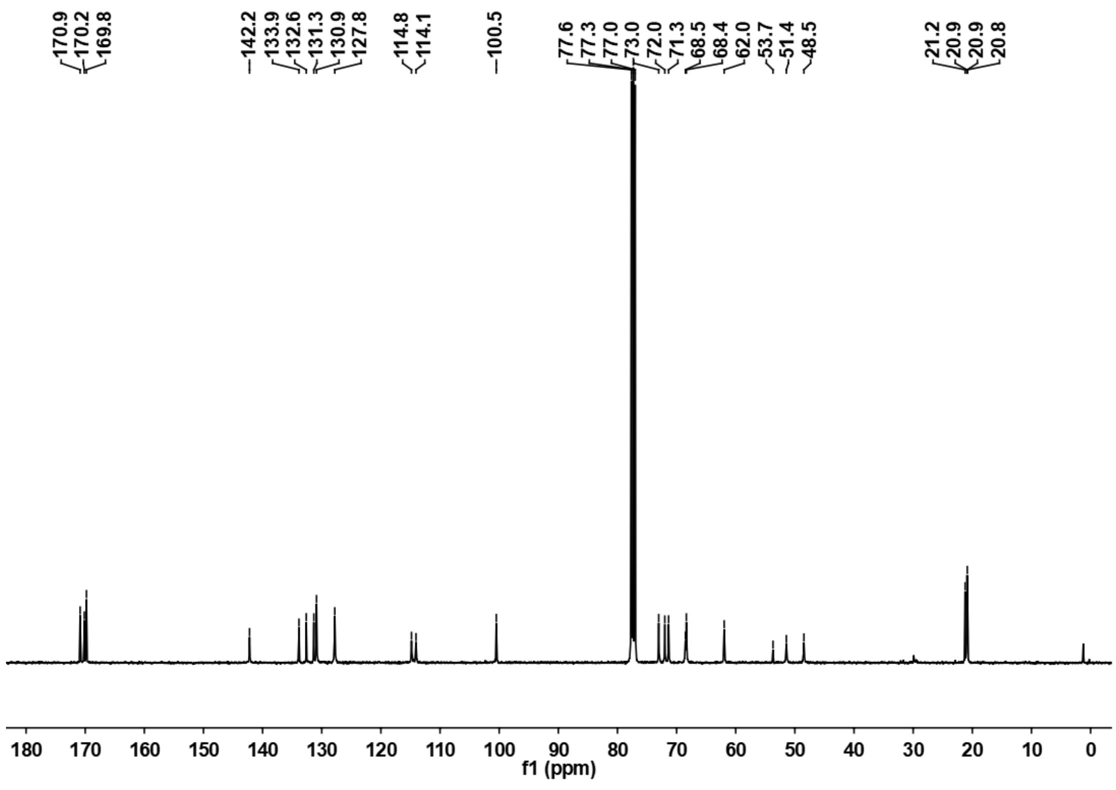

Fig. S45 ^{13}C NMR of Cat**1** in $CDCl_3$.

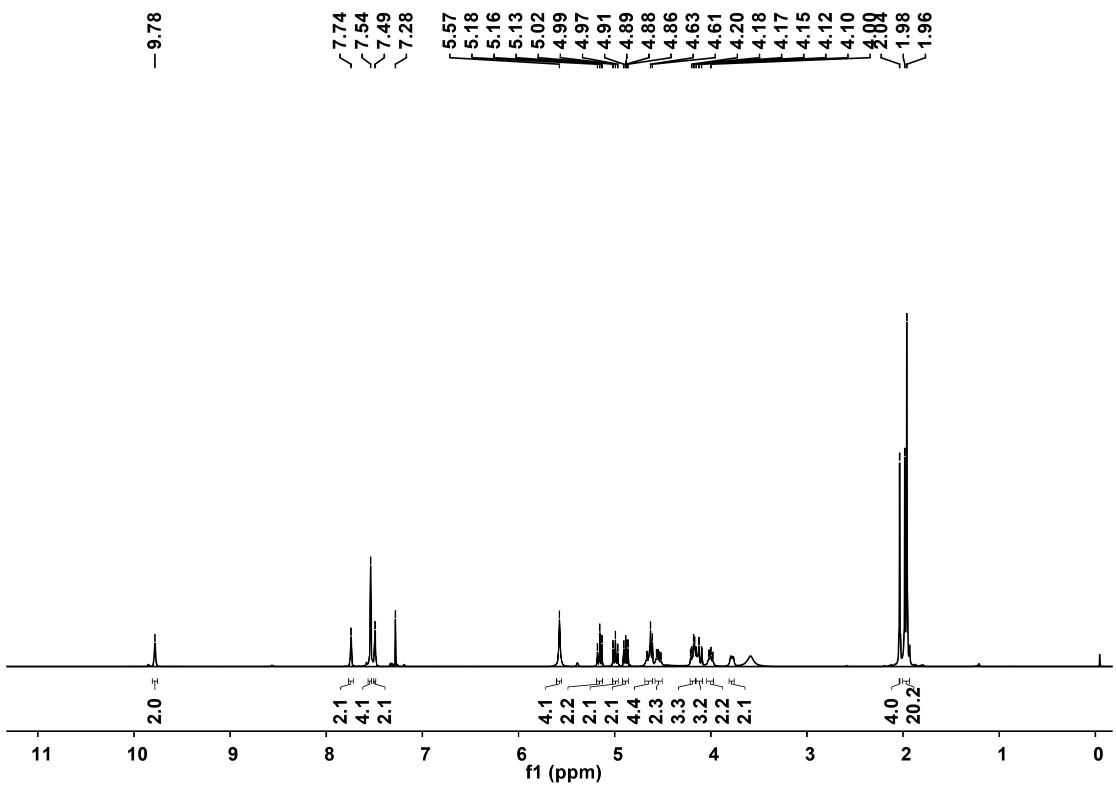

Fig. S46 ^{1}H NMR of Im-Br**2** in $CDCl_3$.

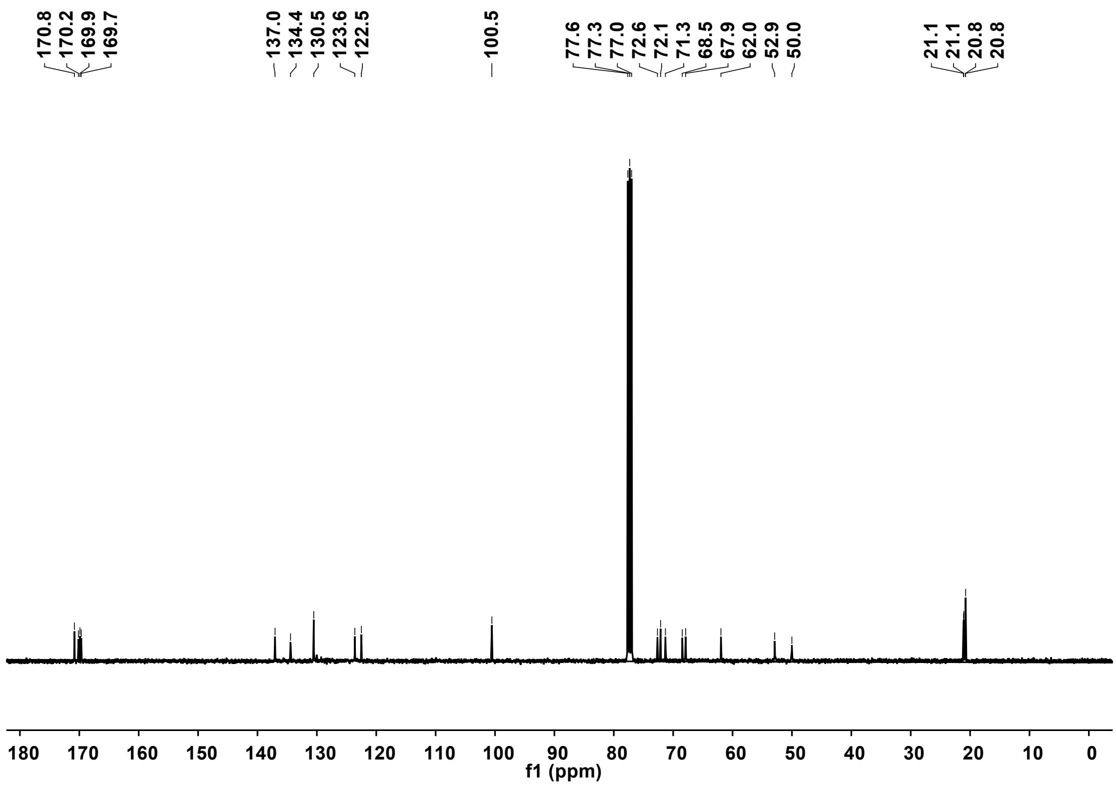

Fig. S47 ^{13}C NMR of Im-Br**2** in $CDCl_3$.

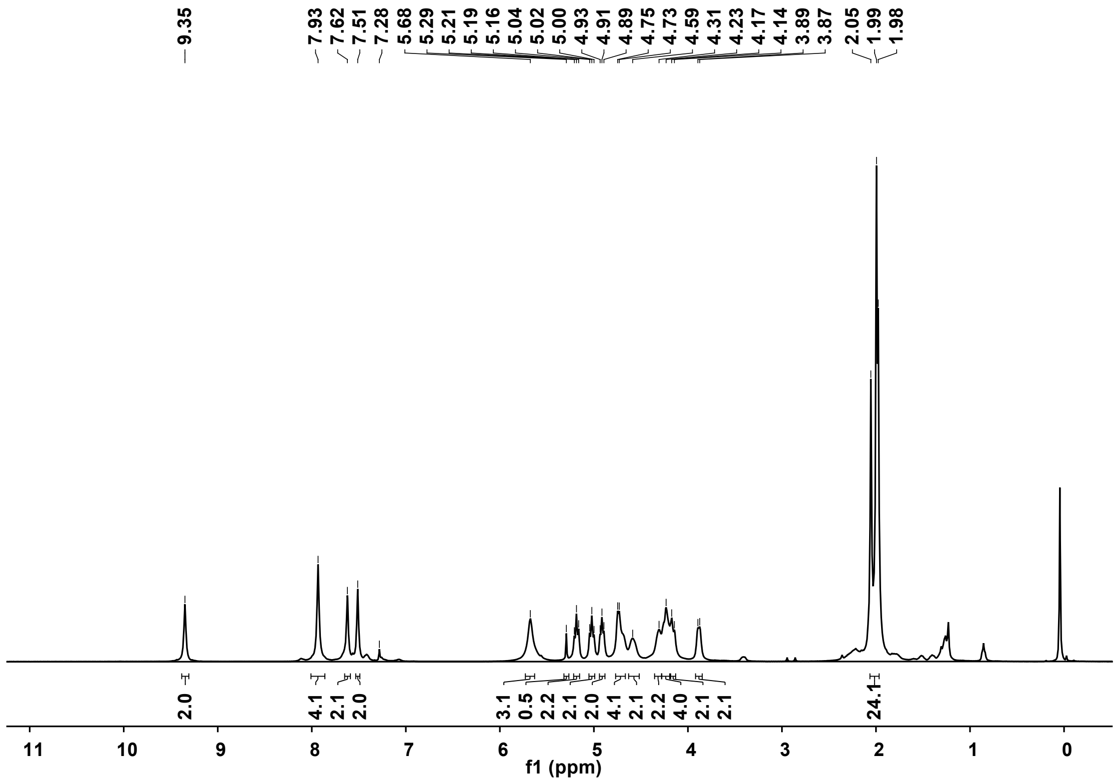

Fig. S48 ^{1}H NMR of Cat**2** in $CDCl_3$.

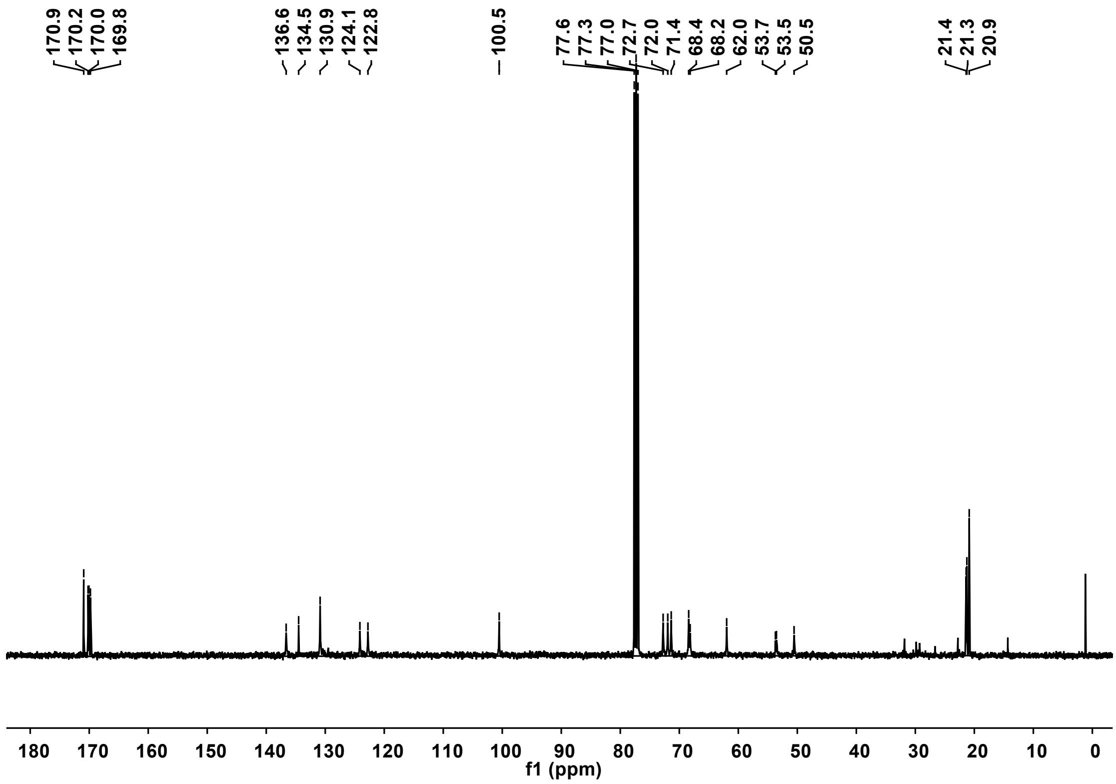

Fig. S49 ^{13}C NMR of Cat**2** in $CDCl_3$.

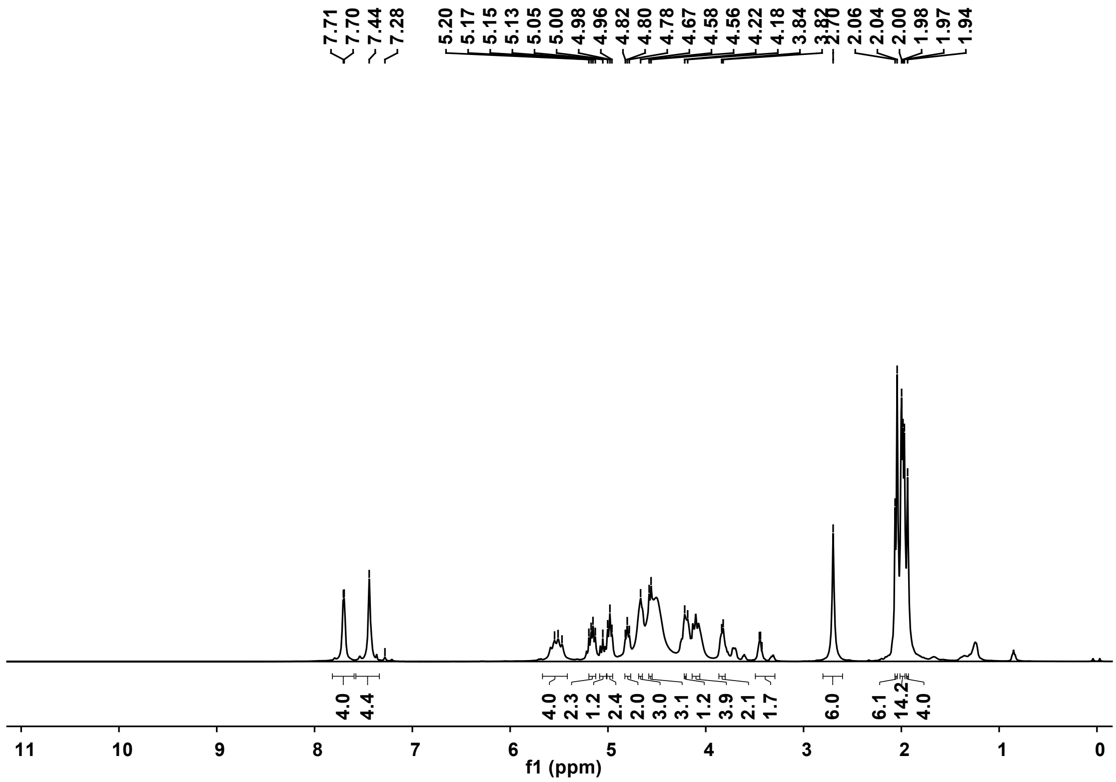

Fig. S50 ^{1}H NMR of Im-Br**3** in $CDCl_3$.

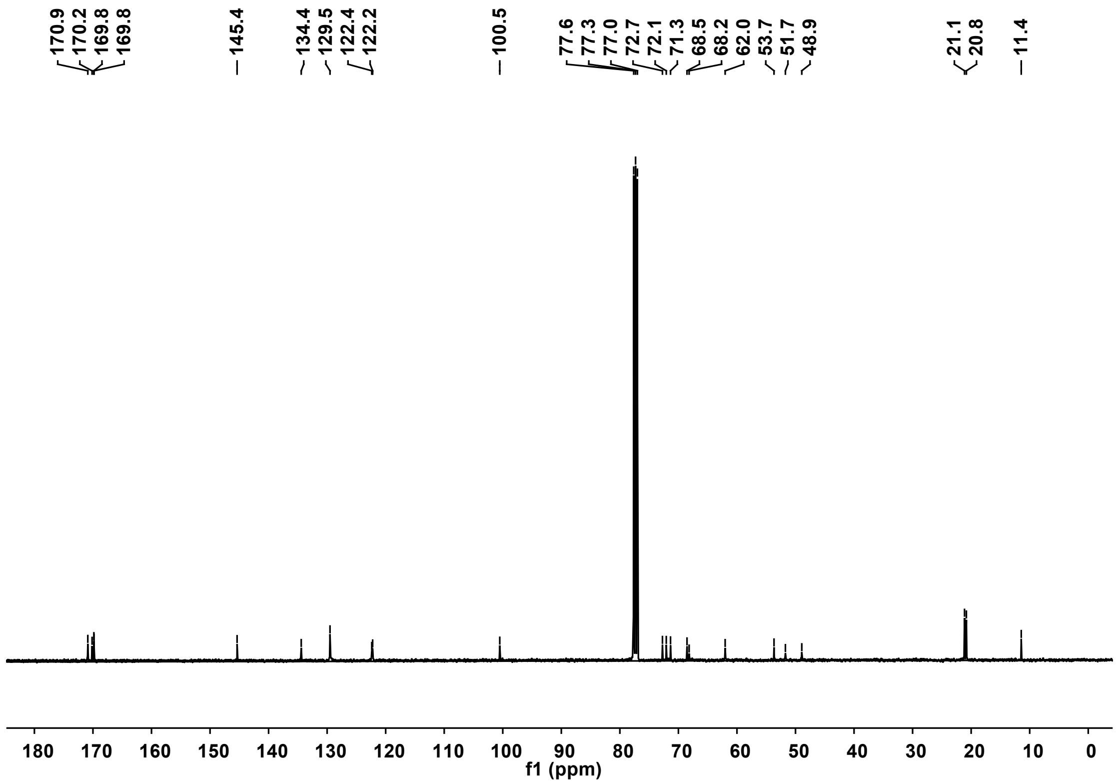

Fig. S51 ^{13}C NMR of Im-Br**3** in $CDCl_3$.

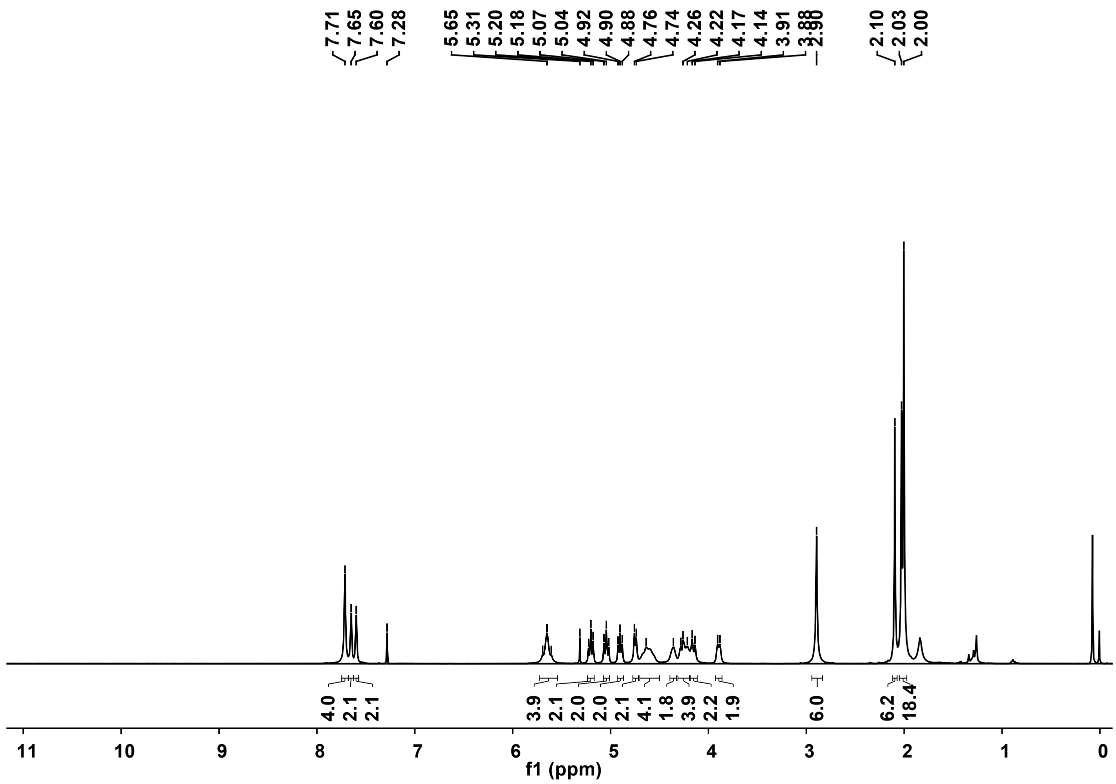

Fig. S52 ^{1}H NMR of Cat**3** in $CDCl_3$.

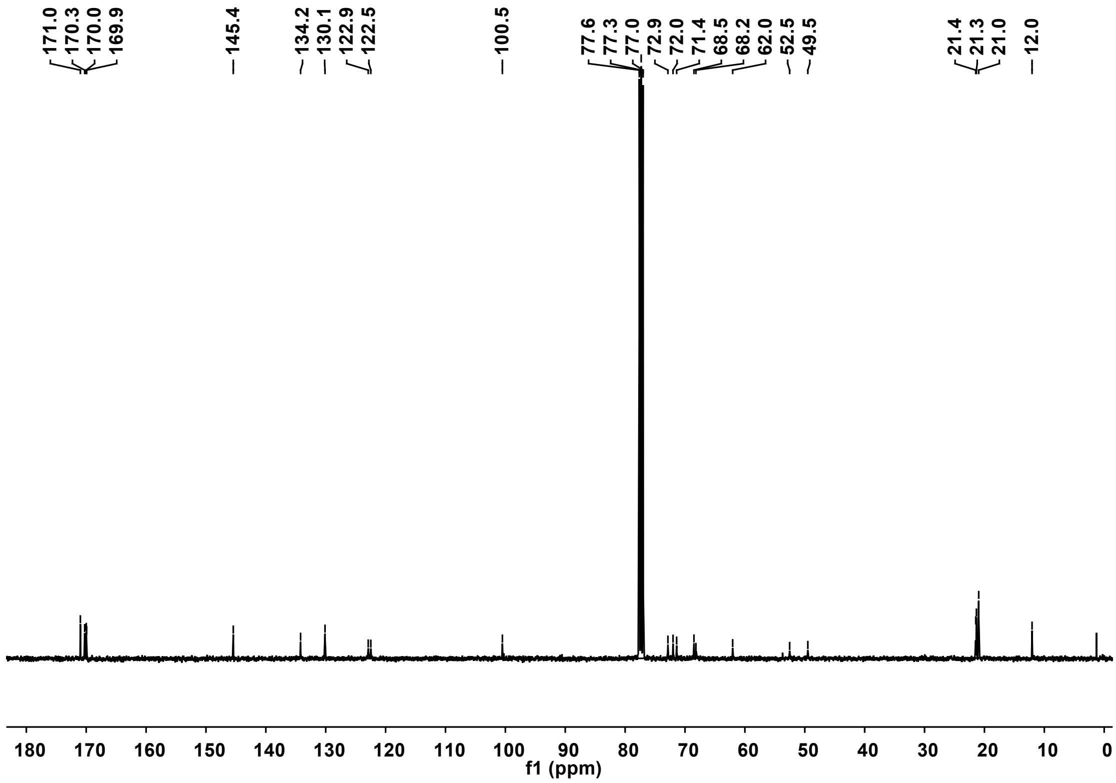

Fig. S53 ^{13}C NMR of Cat**3** in $CDCl_3$.

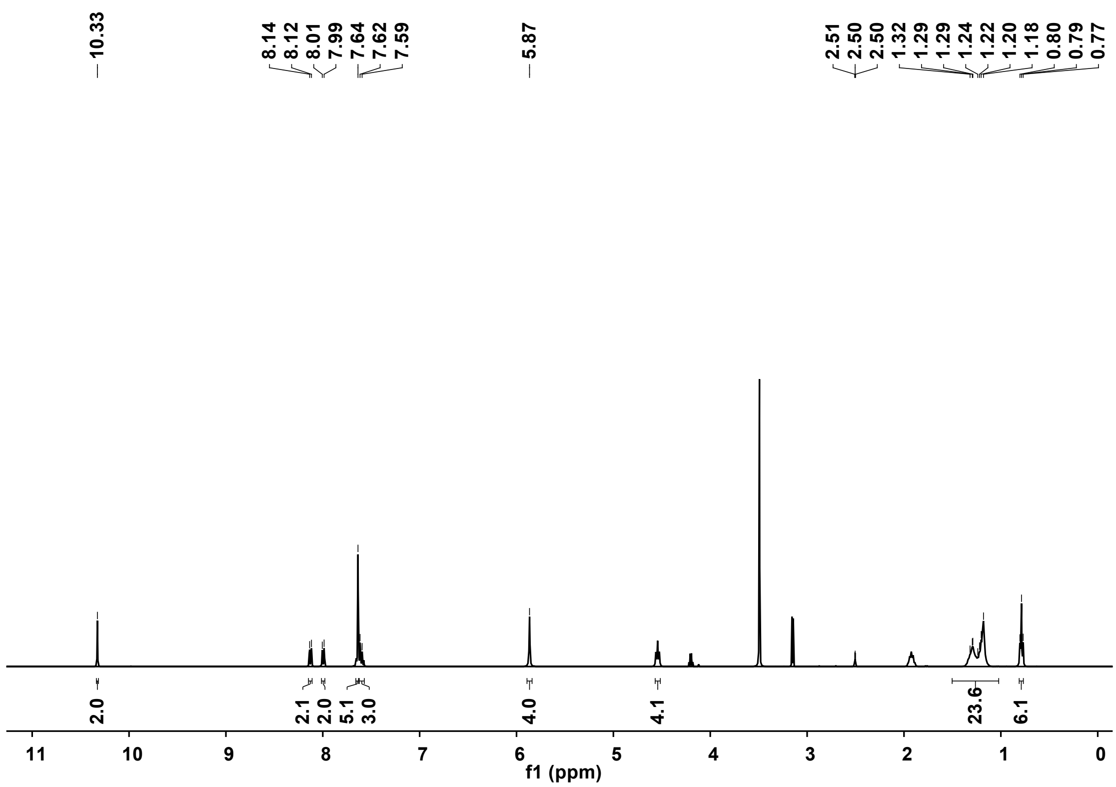

Fig. S54 ^{1}H NMR of Im-Br**4** in DMSO-d_6.

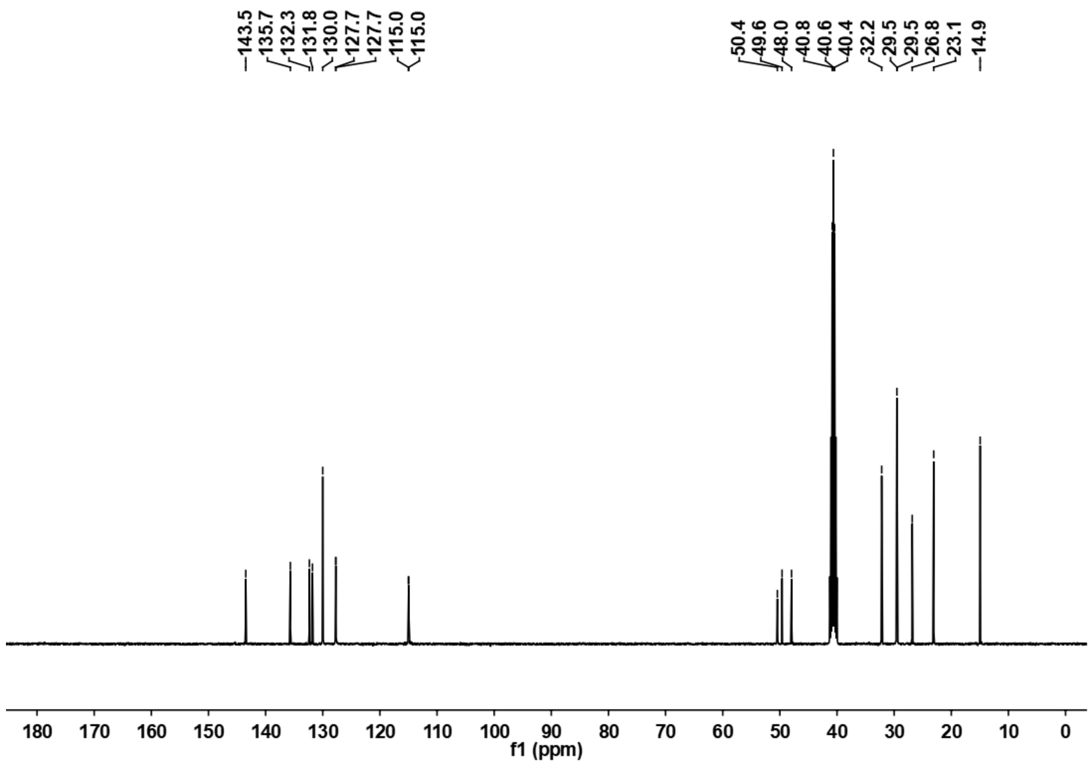

Fig. S55 ^{13}C NMR of Im-Br**4** in DMSO-d_6.

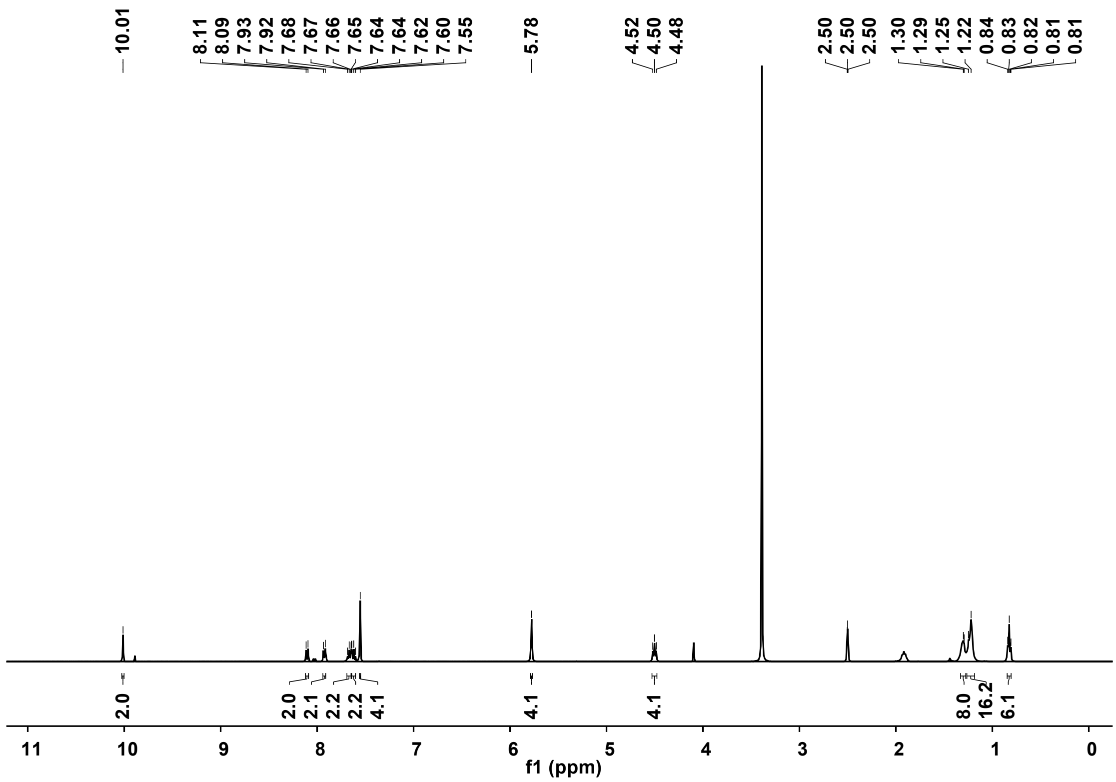

Fig. S56 [1]H NMR of Cat**4** in DMSO-d_6.

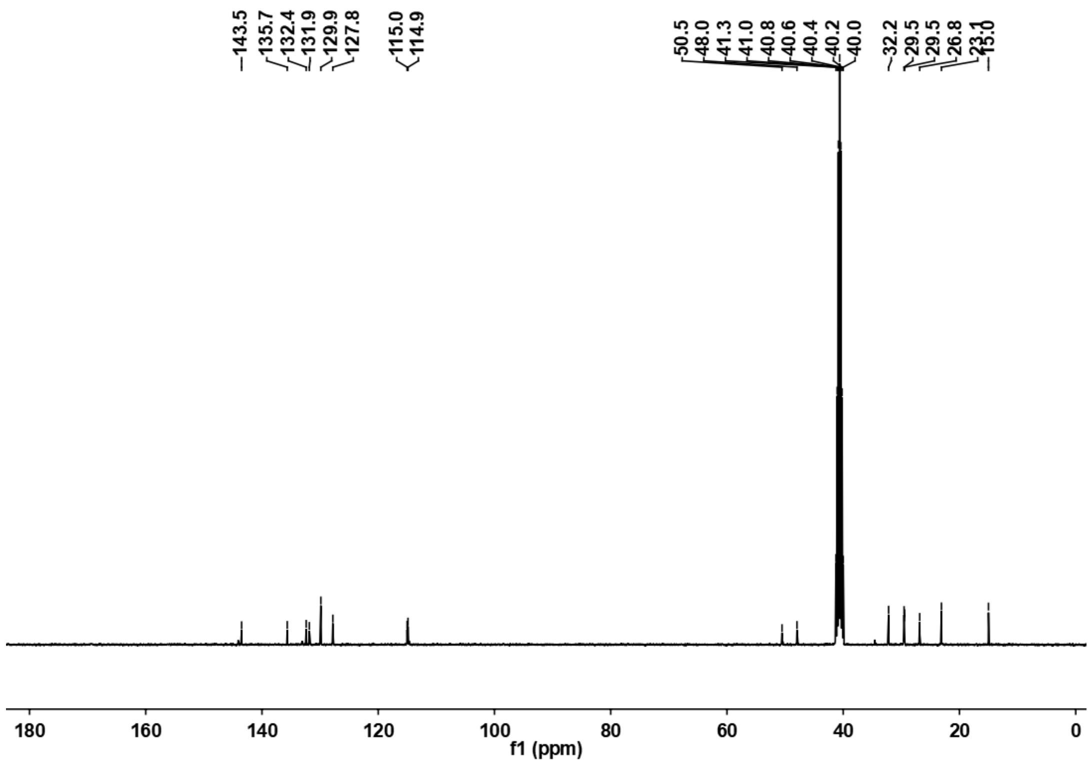

Fig. S57 [13]C NMR of Cat**4** in DMSO-d_6.

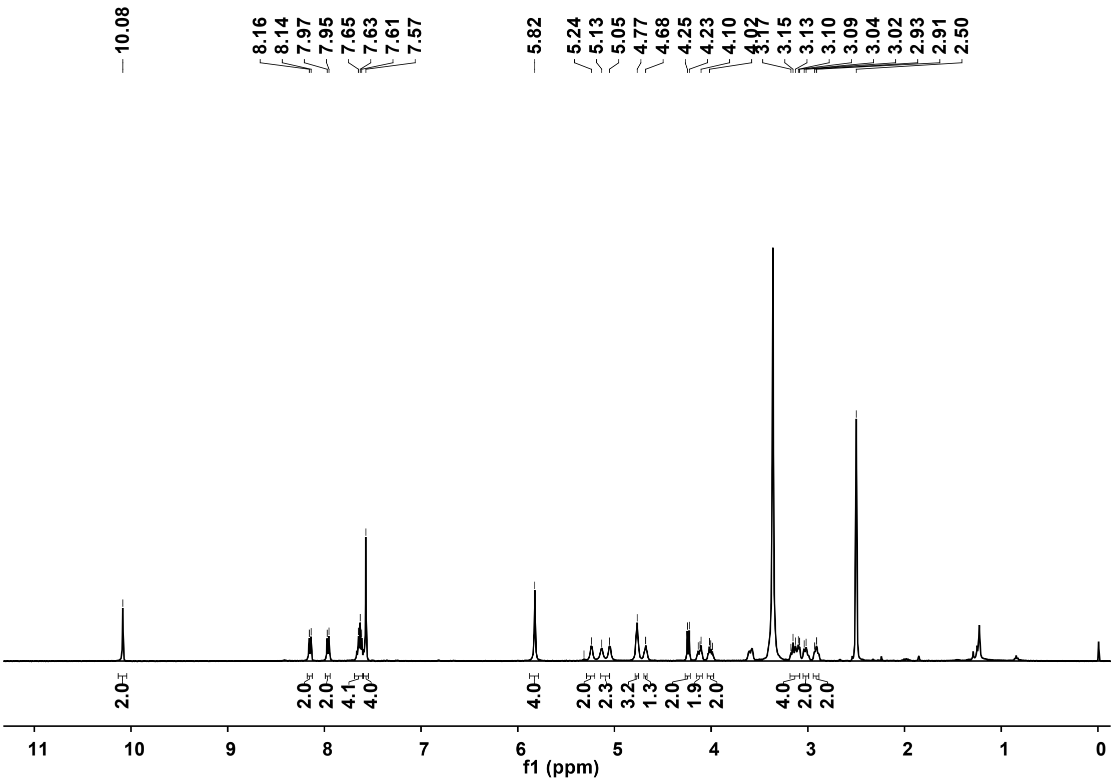

Fig. S58 ^{1}H NMR of Im-Br**5** in DMSO-d_6.

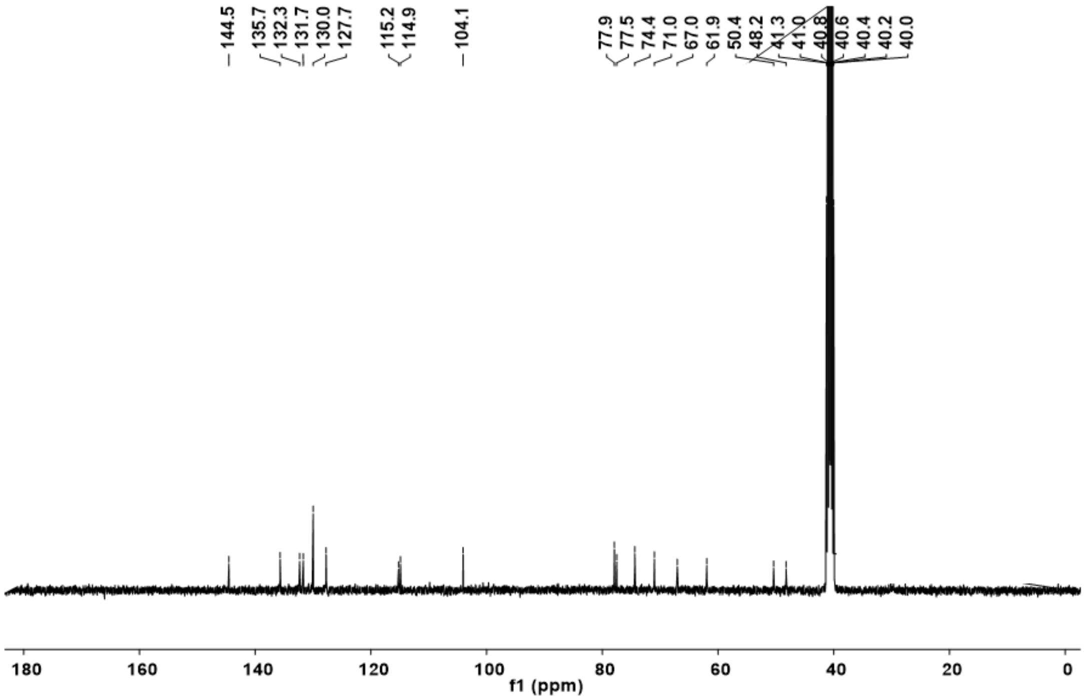

Fig. S59 ^{13}C NMR of Im-Br**5** in DMSO-d_6.

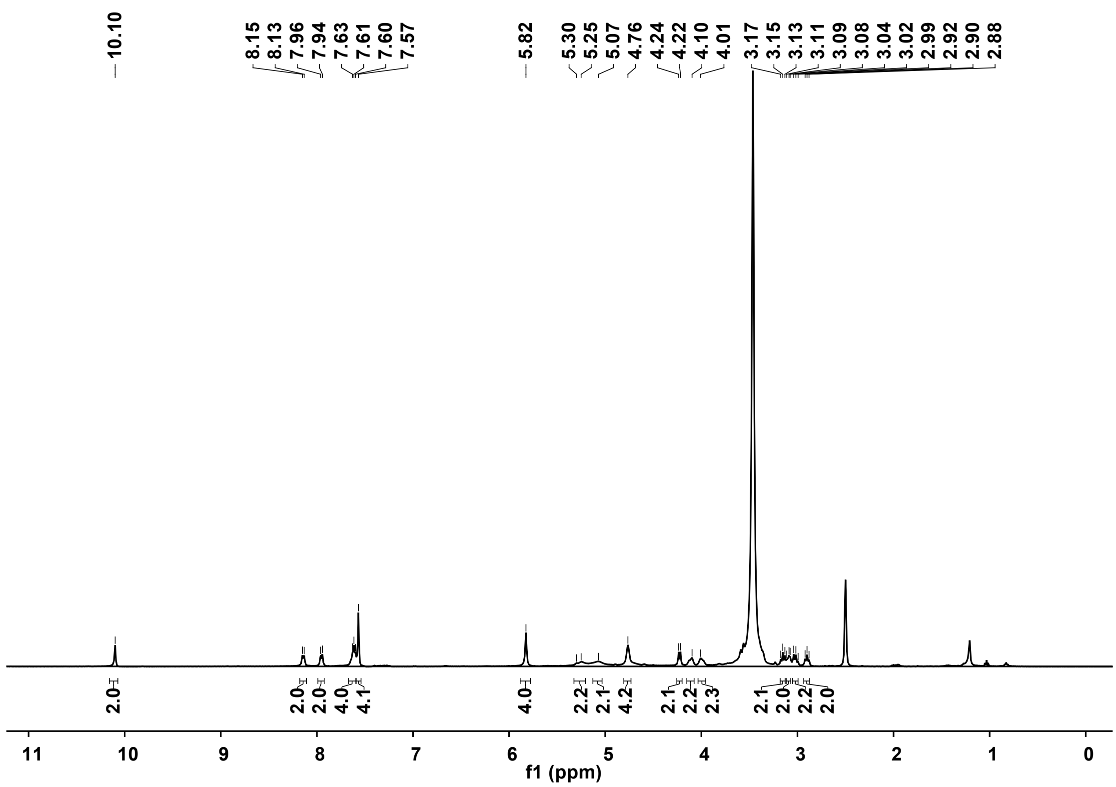

Fig. S60 ^{1}H NMR of Cat**5** in DMSO-d_6.

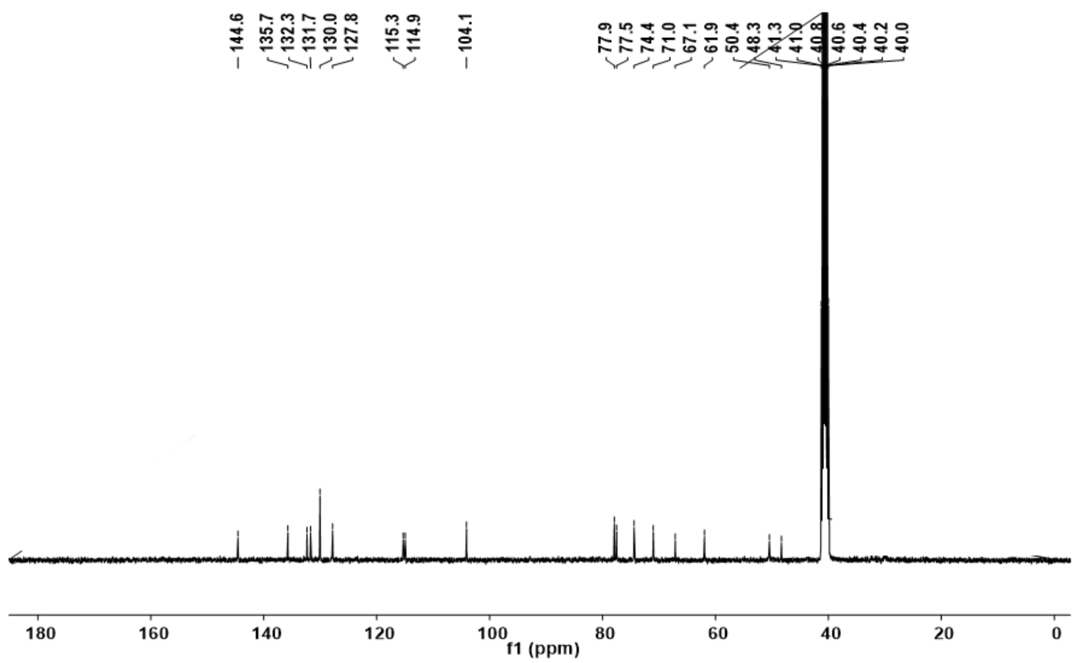

Fig. S61 ^{13}C NMR of Cat**5** in DMSO-d_6.

8. References

1. Y. Zhao, J. Qiu, L. Tian, Z. Li, M. Fan and J. Wang, *ACS Sustainable Chem. Eng.*, 2016, **4**, 5553-5560.
2. Y. Shunsuke, F. Kosuke, K. Satoshi and Y. Tohru, *Chem. Lett.*, 2009, **38**, 786-787.
3. M. Yoshida, T. Mizuguchi and K. Shishido, *Chem. Eur. J.*, 2012, **18**, 15578-15581.
4. Z.-H. Zhou, S.-M. Xia, S.-Y. Huang, Y.-Z. Huang, K.-H. Chen and L.-N. He, *J. CO_2 Util.*, 2019, **34**, 404-410.
5. X. Liu, M.-Y. Wang, S.-Y. Wang, Q. Wang and L.-N. He, *ChemSusChem*, 2017, **10**, 1210-1216.
6. M. Zhao, S. Huang, Q. Fu, W. Li, R. Guo, Q. Yao, F. Wang, P. Cui, C.-H. Tung and D. Sun, *Angew. Chem. Int. Ed.*, 2020, **59**, 20031-20036.
7. Z. Chang, X. Jing, C. He, X. Liu and C. Duan, *ACS Catal.* , 2018, **8**, 1384-1391.
8. C.-S. Cao, S.-M. Xia, Z.-J. Song, H. Xu, Y. Shi, L.-N. He, P. Cheng and B. Zhao, *Angew. Chem. Int. Ed.*, 2020, **59**, 8586-8593.
9. P. Brunel, J. Monot, C. E. Kefalidis, L. Maron, B. Martin-Vaca and D. Bourissou, *ACS Catal.*, 2017, **7**, 2652-2660.
10. S. Ghosh, R. A. Molla, U. Kayal, A. Bhaumik and S. M. Islam, *Dalton Trans.*, 2019, **48**, 4657-4666.
11. Y. Zhang, X. Lan, F. Yan, X. He, J. Wang, L. Ricardez-Sandoval, L. Chen and G. Bai, *Green Chem.*, 2022, **24**, 930-940.
12. A.-L. Gu, Y.-X. Zhang, Z.-L. Wu, H.-Y. Cui, T.-D. Hu and B. Zhao, *Angew. Chem. Int. Ed.*, 2022, **61**, e202114817.
13. X. L. Jiang, Y. E. Jiao, S. L. Hou, L. C. Geng, H. Z. Wang and B. Zhao, *Angew. Chem. Int. Ed.*, 2021, **60**, 20417-20423.
14. S. Ghosh, S. Riyajuddin, S. Sarkar, K. Ghosh and S. M. Islam, *ChemNanoMat*, 2020, **6**, 160-172.
15. S. Hase, Y. Kayaki and T. Ikariya, *ACS Catal.*, 2015, **5**, 5135-5140.
16. S. Hase, Y. Kayaki and T. Ikariya, *Organometallics*, 2012, **32**, 5285-5288.
17. F. Inagaki, K. Maeda, K. Nakazawa and C. Mukai, *Eur. J. Org. Chem.*, 2018, **2018**, 2972-2976.
18. F. Inagaki, K. Maeda, K. Nakazawa and C. Mukai, *J. Org. Chem.*, 2018, **2018**, 2972-2976.
19. X. Wang, Z. Chang, X. Jing, C. He and C. Duan, *ACS Omega*, 2019, **4**, 10828-10833.
20. K.-i. Fujita, K. Inoue, J. Sato, T. Tsuchimoto and H. Yasuda, *Tetrahedron*, 2016, **72**, 1205-1212.

21. Z.-G. Zhou, P. He, J. Li, J. Zhang, G. Xu, S.-Y. Zhang, X.-X. Deng, Z.-Y. Du, G.-T. Luo, H.-Y. Zhen, Y. Chen and C.-T. He, *Org. Chem. Front.*, 2023, **10**, 2045-2053.
22. L. Li, Y. Lv, H. Sheng, Y. Du, H. Li, Y. Yun, Z. Zhang, H. Yu and M. Zhu, *Nat. Commun.*, 2023, **14**, 6989.
23. W.-Z. Qiao, Y.-J. Wang, S. Li, R. Wang, J. Wu and S.-Q. Zang, *CCS Chemistry*, 2024, **6**, 1-11.
24. X.-J. Zhang, L.-F. Kong, X. Lu, Y.-L. Liu, Y. Hu, H.-W. Gong, Y.-J. Li and Z.-G. Zhou, *J. Carbohydr. Chem.*, 2024, **42**, 180-196.
25. J. Qiu, X. Qi, K. Zhu, Y. Zhao, H. Wang, Z. Li, H. Wang, Y. Zhao and J. Wang, *Green Chemistry*, 2024, DOI: 10.1039/d4gc00122b.
26. Q. Cao, W. Sun, Z. Xiao, X. Zhou, L. Lu, H. Hou, Y. Chen and L. Wang, *Small*, 2024, DOI: 10.1002/smll.202404202, e2404202.